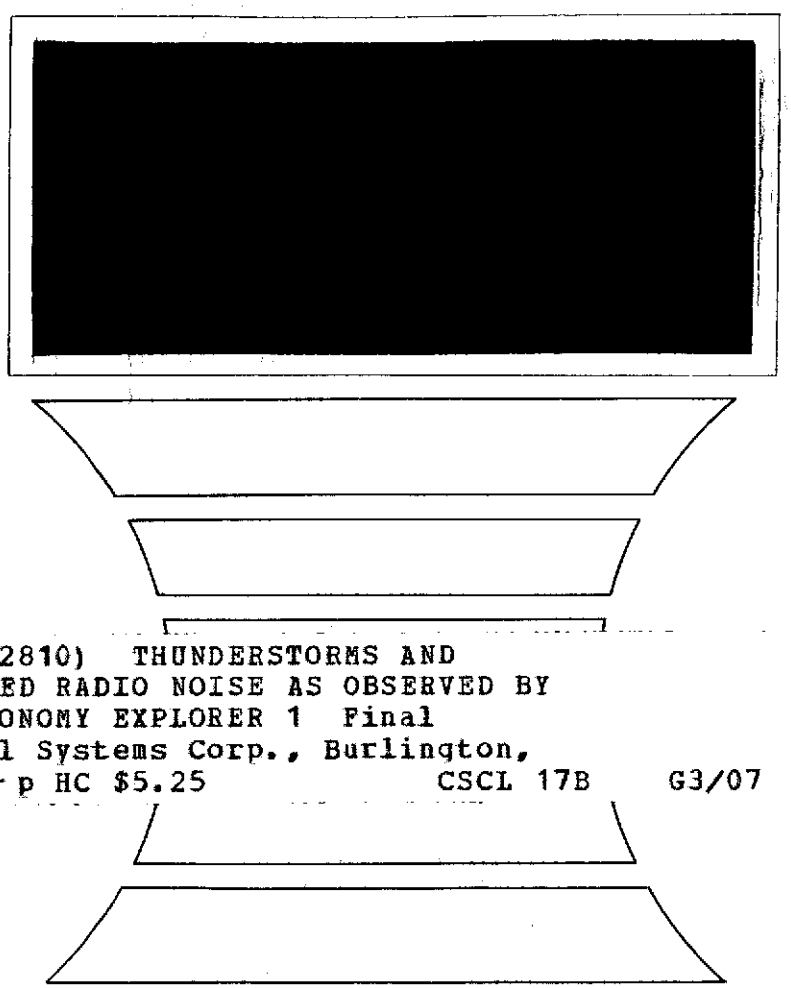

NASA-CR-132810) THUNDERSTORMS AND GROUND-BASED RADIO NOISE AS OBSERVED BY RADIO ASTRONOMY EXPLORER 1 Final (Analytical Systems Corp., Burlington, Mass.) 64 63 p HC $5.25 CSCL 17B G3/07

N73-32062

Unclas 18208

Analytical
Systems Engineering
CORPORATION

25 RAY AVENUE
BURLINGTON, MASSACHUSETTS 01803

Analytical
Systems Engineering CORPORATION

25 RAY AVENUE
BURLINGTON, MASSACHUSETTS 01803
(617) 272-7910

THUNDERSTORMS AND GROUND-BASED RADIO NOISE AS OBSERVED BY RADIO ASTRONOMY EXPLORER 1

BY

JOSEPH A. CARUSO AND JOHN R. HERMAN

ANALYTICAL SYSTEMS CORPORATION
25 RAY AVENUE
BURLINGTON, MASSACHUSETTS 01803

APRIL 5, 1973

Final Report on Contract NA55-23121

Period Covered: May 18, 1972 to November 17, 1972

Prepared for:

NATIONAL AERONAUTICS AND SPACE ADMINISTRATION
Goddard Space Flight Center
Greenbelt, Maryland 20771

ABSTRACT

Radio Astronomy Explorer (RAE) I data are analyzed to determine the frequency dependence of HF terrestrial radio noise power. RAE observations of individual thunderstorms, mid-ocean areas, and specific geographic regions for which concommitant ground based measurements are available indicate that noise power is a monotonically decreasing function of frequency which conforms to expectations over the geographic locations and time periods investigated. In all cases investigated, active thunderstorm regions emit slightly higher power as contrasted to RAE observations of the region during meteorologically quiet periods. Noise levels are some 15 dB higher than predicted values over mid-ocean, while in locations where ground based measurements are available a maximum deviation of 5 dB occurs. Worldwide contour mapping of the noise power at 6000 km for five individual months and four observing frequencies, examples of which are given in the report, indicate high noise levels over continental land masses with corresponding lower levels over ocean regions.

ACKNOWLEDGEMENTS

We are indebted to several people for their cheerful assistance and helpful discussions throughout the course of this work. Mr. J. Musser (Analytical Systems Engineering Corporatic provided illuminating comments on radiowave propagation and a set of nomographs derived from K. Davies' book to facilitate manual ray tracing.

Several lively discussions of the concepts presented in this report were held with Mr. R. Vargas-Vila (ASEC). Mr. Richard Tolini (ASEC) read microfilmed data until his eyeballs flashed red, and he transfered most of the data points to base maps for subsequent noise contouring.

Our thanks go to Mr. R. T. Disney (NOAA) for providing ground-based noise measurements at Pretoria, Africa and Cook, Australia as well as discussions concerning their collection and processing within the context of how they fit into the correlative analysis reported here.

Dr. R. G. Stone (NASA Goddard) provided a continuing source of encouragement and valuable technical guidance in all aspects of the work, for which we are sincerely grateful.

Table of Contents

1.0 Introduction

In addition to providing significant measurements of galactic and solar radiation since July 1968, the utility of the Radio Astronomy Explorer (RAE) I Satellite has been further enhanced during the past two years as a result of its capability to provide global coverage of the Radio Noise Environment in near space (6000 KM), having its genesis in terrestrial noise sources. RAE's potential as a means of globally monitoring terrestrial radio noise in a continuous manner was recognized early, but it has been only recently that scientists have begun to investigate this aspect of the RAE measurements. Consequently, RAE's potential in this most interesting and important area has not been fully exploited.

Preliminary investigations at ASC have been extremely encouraging and the frame work now exists within which to engage in more detailed and expansive studies of the Terrestrial Noise Environment. These preliminary findings have been communicated to the scientific community by means of four symposia presentations (Caruso, et al, 1972 a, b,; Herman, et al, 1972, a,b.).

The objective of the present report is to display the analytical results arrived at under the current contract, (NAS 5-23121), both quantitatively and in descriptive fashion. The development of a simple mathematical model describing the frequency dependence of the noise power is given in Section 2, and the model is then utilized for analysis and comparison of simultaneous ground-based and satellite noise measurements (Section 3).

RAE observations of individual thunderstorm events occurring in the U.S. are discussed in Section 4, and global maps of terrestrial noise on 9.18, 6.55 and 4.7 MHz for December, 1968, and 9.1 MHz for October, 1968, and August, 1969, are presented in Section

Throughout this report, effects of the spatial and temporal variations in ionospheric penetration frequency on the observed noise at RAE altitude are considered, and taken into account quantitatively where appropriate.

The results presented here support and amplify the earlier tentative conclusions derived under Contract NAS 5-11386. Although this document is the "final report" under Contract NAS 5-23121, its contents should be regarded as a technical progress report, for there is still much to be learned from the extensive and valuable data base provided by the RAE I satellite.

2.0 Frequency Dependence of Noise Power

2.1 Elementary Theory

A mathematical formulation of the frequency dependence of the noise power is perhaps an ambitious enterprise in the case of RAE observations of terrestrially generated noise, since the noise power at the satellite is a function of several not easily determined variables in addition to the frequency. In principle, an accurate formulation can be arrived at, not without some difficulty to be sure, if there is sufficiently detailed information at the disposal of the investigator concerning the time dependence of the source intensities and source distributions, the state of the intervening ionosphere, antenna characteristics, meteorological conditions and so forth. Lacking such information, a completely successful, general formulation of the functional relationship between noise power and frequency is not possible. Nevertheless, with certain simplifying assumptions and a judicious choice of RAE location and observational period, a relationship can be derived which correlates very well with earlier theoretical studies, and more importantly, with other independent experimental observations.

A simplified concept of the relationship between the noise at the ground, the intervening ionosphere, and the terrestrial noise at the satellite is shown in Figure 1.

It assumes with flat Earth geometry, that the ground is visible to the satellite at height H over a circular area of radius R, and the noise is uniformly distributed throughout the area. The radius might be fixed by the ionosphere, the antenna area projected to the ground, or the size of the thunderstorm; at present,

it appears that the ionosphere is the dominant factor.

The power flux density incident at the satellite P_s (Wm^{-2} Hz^{-1}), is

$$P_s = \frac{k}{A_s} T_s \qquad (1)$$

where k is Boltzmann's constant, A_s is the RAE antenna aperture, and T_s is the equivalent antenna temperature measured by RAE. Similarly, the power flux density radiated by a point source at the ground is

$$P_g = \frac{kT_g}{A_g} \qquad (2)$$

Now assuming that the energy is radiated isotropically into the half-sphere above the ground, the power flux density at a distance D due to the sources in an elemental area of the extended source (Figure 1) will be

$$dP_s = \frac{P_g \, Rd\theta dR}{2\pi D^2} \qquad (3)$$

where $D^2 = R^2+H^2$ when RAE is vertically above the extended source center.

The total power flux density at the satellite is, then,

$$P_s = \int_0^R \int_0^{2\pi} \frac{P_g \, RdRd\theta}{2\pi (R^2+H^2)} \qquad (4)$$

To make the integration tractable, we have considered only cases where the predicted foF2 contours are of a circular nature surround

ing the area in question. Under these circumstances, the expression can be integrated directly with the following result;

$$P_s = \frac{1}{2} P_g \log_e \left(\frac{R^2+H^2}{H^2}\right) \qquad (5)$$

Since the effective antenna area is

$$A = \frac{\lambda^2 G}{4\pi}$$

where G is the gain and λ the wavelength, eqs. 1, 2 and 5 combine to form

$$T_s = \frac{1}{2} T_g G_s \log_e \left(\frac{R^2+H^2}{H^2}\right) \qquad (6)$$

where T_g now is the temperature which would be measured at the ground with an omnidirectional antenna ($G_g = 1$), and G_s is the gain of the RAE antenna.

If ionospheric refraction is neglected and the ionosphere is assumed to have a critical frequency of f_c and a virtual height of 300 km, the relationship between the ratio of critical to observing frequency (f) and the great circle distance (L) between a point source and the subsatellite point can be shown to be (Herman, et al, 1973)

$$\frac{f_c}{f} = \left[1 - \frac{\sin^2 (L/R_e)}{1.39-1.14 \cos (L/R_e)}\right]^{1/2} \qquad (7)$$

where R_e = 6370 km, the Earth's radius.

For a spatially constant critical frequency or an ionosphere concentric about the subsatellite point, L=R, so that the effec-

tive viewing area can be deduced from a knowledge of the critical frequency distribution.

To summarize the limitations to equation 6; (a) the source temperature is probably not constant over the whole viewing area, so T_g represents the average of the temperatures that would be measured by placing an omnidirectional antenna at a number of locations within the viewing area; (b) because R equals the satellite horizon (∿6500 km) with no ionosphere the flat Earth approximation breaks down when the critical frequency is sufficiently low; (c) the viewing area is circular only when the critical frequency throughout the viewing area is either constant or concentrically distributed about the subsatellite point.

The events selected for the analysis are within limitations (b) and (c), but the results are necessarily the average ground noise temperature over the whole viewing area.

2.2 Application to Ocean Control Passes

In order to test the usefulness of the model and also to establish what the noise level is during meteorologically quiet conditions, a number of RAE orbits over the central Atlantic and northern Pacific Oceans where selected for study. The choice of ocean regions is based on the fact that they are well removed from man made noise sources and transmitters, almost all of which are located on continental land masses. A further consideration is that there is a low probability of thunderstorm occurrence over the major oceans (Crichlow, et al, 1971). Consequently, the noise power as a function of frequency over the Pacific and Atlantic

can be used as a standard or guide from which to measure the increase in noise power from man made sources and atmospheric noise. The results of control day passes over the Atlantic and Pacific Oceans during selected time periods in September, 1969 are depicted in figure 2. The computations of source temperature were made using equations (6) and (7), Section 2.1. The predicted values of critical frequency at the geographic locations and times under investigation indicate that the ionosphere is reasonably concentric. Therefore, $L \simeq R$ is the radius of the satellite viewing area. Using the predicted values of critical frequency to establish the variability of R and the measured values of T_s, the average ground temperature T_g beneath the viewing area was calculated using Equation (6) for each frequency. The most prominent features of the curves are the monotonic decrease of noise power with frequency and the fact that the measured curves are some 15 db higher than predicted noise factors. Since predictions over ocean areas are somewhat less reliable than in those areas where the predicted values can be weighted on the basis of noise measurements, i.e. on land, it is reasonable to conclude that the disparity in the curves is a result of the predictions being too low.

The fact that the shape of the measured noise power curve conforms to what one would expect on the basis of our prior knowledge of the frequency dependence of the noise lends credibility to the model developed. As will be shown in Section 3, the difference in the magnitude of the noise which in this case is 15 db is reduced to a negligible amount when the RAE observations are compared to ground based measurements.

3.0 Comparison With Ground Based Measurements

In order to ascertain what fraction of the total energy intercepted by RAE's lower VEE antenna has its origin in a region directly below the satellite, a comparison between RAE and ground based measurements on ARN-2 receivers (short vertical whip antennas) located at Cook, Australia and Pretoria, South Africa was carried out. Attention is focused on Pretoria since, in this case, a quite interesting phenomenon manifests itself, although in all other particulars the results at Cook and Pretoria are equivalent.

The radiation from below the satellite may be due to direct thunderstorm contributions, man-made noise, ground based transmitter located within the satellite viewing area and operating with the 200 khz RAE band width, or the radiation can be due to contributions from distant sources arriving in the area via ionospheric reflection

Certainly, another possibility is that distant transmitters are, in fact, a major contributor to the total noise power at the satellite, propagating energy either directly or via ionospheric reflections penetrating the ionosphere from areas other than directl below the satellite.

It is shown later that this possibility is very small when the transmitter is sufficiently far away. It is reasonable to assume that, based on the inter-relationship between the location of terrestrial noise sources, the ionosphere, and the satellite position and antenna pattern, each measured value of noise temperature should be plotted at a geographic position directly below the satellite corresponding to the time of measurement. The validity of this assumption is strengthened because of the good correlation between the contour maps discussed in Section 5 and what we

are led to believe by prior knowledge of the spatial and temporal distribution of noise sources, transmitter locations, the ionosphere, and CCIR predictions among other things.

The Raison d'Etre of the comparison with ground based measurements is to further investigate the validity of this assumption in a more direct manner. To this end, records of ground based ARN-2 receiver measurements taken at Cook and Pretoria were acquired from Mr. Robert Disney (NOAA) for selected periods during 1969.

In order to make this comparison, the model developed to derive the noise power versus frequency dependence in Section 2 was employed in conjunction with manual ray tracing techniques discussed by Davies (1965) to determine the direct contribution from distant sources.

As an illustration of the results obtained on the basis of the satellite viewing area model and the manual ray tracing analysis, an RAE pass over Pretoria, South Africa on July 20, 1969 at 1741UT (1900LT) is investigated in some detail.

This pass was selected because RAE was directly over Pretoria during local evening where the measured value of foF2 at Pretoria, 3.4 MHz, indicated that the ionosphere was transparent to the observing frequencies. Further considerations are that the predicted and measured values of foF2 were reasonably close and the foF2 contours display a circular character in the area surrounding Pretoria. Directly south of Pretoria foF2 decreases and the viewing area is larger and non-circular.

We have constrained the area to be circular in this direction. This is reasonable since the region toward the pole and over southern ocean areas are regions of low noise activity well outside the main

beam of the antenna and, therefore, will represent at best a second order contribution to noise power.

The noise temperature of the RAE lower antenna as a function of universal time as RAE passed over Pretoria is shown in Figure 3. The curves are parametric in frequency. At 1738UT, Pretoria is just within the perimeter of the RAE viewing area, as RAE approaches. The noise temperature has saturated the receiver on 3.93 MHz but we can at least set a lower limit of 10^{10} ^{o}K. The temperatures on the remaining frequencies decrease with decreasing frequency.

At approximately 1741UT, RAE is directly over Pretoria. The noise temperature on 3.93 MHz has fallen considerably, and the temperature decreases with decreasing frequency for all observing frequencies. At 1750UT, RAE has moved away, but Pretoria is still withi the perimeter of the viewing area and the noise temperature on 3.93 MHz has increased to 2×10^{9} ^{o}K, while the values on 4.7 to 9.18 MHz are essentially the same as they were at 1741UT. Figure 4 will be of some assistance in the visualization of the viewing area location at the times mentioned above.

The data shown in Figure 3 is simply the total noise temperature as measured at the satellite. When the circular viewing area as determined by the local critical frequency and observing frequency is taken into account in the manner prescribed by the model developed earlier, one arrives at the results displayed in Figure 5. Noise factor is plotted as a function of frequency at 1741UT. The CCIR (1964) predicted values and the ground based measurements, (Disney, private communication) are plotted in addition to the RAE measurements. Correlation between the ARN-2 and RAE measurements

is very good, the maximum deviation being about 4 dB. The fact that the CCIR predictions are lower is very likely a result of the values being averaged over a number of months and over a four hour time period.

The situation is significantly different at 1738UT as indicated in Figure 6. Fa at 3.93 MHz is >75 dB. This anomalous behavior at 3.93 MHz can be accounted for in the following way: The International Frequency Registration Board lists four transmitters in Johannesburg, adjacent to Pretoria, operating within the RAE band width centered at 3.93 MHz. These are the only transmitters operating on any of the observing frequencies within the viewing area, as far as we can ascertain. The combined total radiated power, assuming 10% efficiency, ranges from 8 to 40 kw.

A calculation of the loss incurred over the propagation path from the transmitters to RAE indicates that a temperature of about 10^{13} ^{o}K should be measured at the satellite, and this would clearly explain the noise factor being in excess of 75 dB. For the satellite viewing area directly over Pretoria at 1741UT, RAE would be directly above a null of the antenna and, therefore, the transmitters would not contribute significantly.

At 1750UT as RAE moves away from Pretoria, the noise factor on 3.93 MHz is 68 dB.(Fig.7) This is reasonable if it is assumed that the antenna has some directivity toward the central and northern parts of the continent and lower radiated power southward toward the pole.

The phenomenon of noise power fading as RAE passes directly over either isolated, known transmitter locations, or localized clusters of transmitters as in this case in Northern China, recurs often enough to indicate that the phenomenon is not a chance occurrence.

A further example of power fading over the cluster of 9180 ± 20 KHz transmitters in Northern China is depicted in Figure 8 .

As suggested earlier, distant transmitters may make major contributions either directly or via ionospheric reflections penetrating the ionosphere from areas other than directly below. Figure 9 indicates the geometry involved and some limiting cases resulting from ray tracing application. The transmitters operating at about 9.18 MHz are located at Urumschi, China (Sinkiang Province) and the satellite is located directly above Pretoria at 1741UT. The great circ path is divided into 1000 km increments and labeled with the appropriate predicted value of foF2.

For the 1 1/2 hop case, an examination of the figure in the region where the ray would penetrate the ionosphere, and an application of Snell's Law indicates the ray would be unable to penetrate. This is also true for the 7 1/2 hop case. Thus, we can conclude that there are no paths to RAE via reflections and penetration from areas other than below the satellite.

Although it is possible that some direct path might exist from t transmitters, the ray tracing technique used is unable to calculate just how much energy will arrive via such a direct path. However, the good correlation shown in the earlier figures between the ground based and satellite observations indicate that it should be small. But perhaps even more importantly, at times when RAE is on the dayside where the ionosphere would be expected to effectively shield the noise sources directly below the satellite radiating at the RAE observing frequencies, the noise temperature on the lower Vee is invariably equal to, or less than that on the Upper Vee, that is,

the terrestrial noise power is always below the cosmic noise background. Since in principle a direct path might exist between RAE and distant transmitters the most obvious, and indeed we feel, the only proper conclusion to be drawn is that energy arriving at the satellite via long direct paths simply does not exceed the cosmic noise background, and does not represent a significant contribution to the total noise power at the satellite.

To summarize, the model developed for radiation from an extended source, when applied to the RAE observations yields good agreement with ground based measurements. The anomalous behavior on 3.93 MHz was accounted for by the presence of 3.93 MHz transmitters located in the viewing area. Ray tracing shows that energy from distant transmitters is unable to reach RAE, in this case, via reflection and penetration from areas outside the viewing area directly below the satellite.

4.0 Individual Thunderstorm Analysis

The detection and monitoring of thunderstorms by an orbiting satellite has been a promising possibility for a number of years. Horner (1965) showed that significant amounts of radio energy from lightning discharges in a thunderstorm area can be expected up to altitudes of about 1000 km. However, there are some major difficulties in using radio techniques for thunderstorm observations by satellite (Pierce, 1969). For the RAE I Satellite in particular, although the directive gain of the VEE antennas is high, the projected antenna beam width from a height of 6000 km constrains RAE to view a very large area relative to individual thunderstorm dimensions. The purpose of our analysis has been to ascertain whether the RAE antenna and orbital parameters yield sufficient terrestrial space resolution for the purposes of thunderstorm detection.

The basic objective of the analysis is to determine the difference in received noise power (expressed as equivalent antenna temperature in ^{o}K) on RAE passes over a given region with and without thunderstorms, as a function of frequency.

Approximately 200 thunderstorms occurring in the U.S. during May through September, 1969, were located utilizing storm data from the World Data Center (WDC) in Ashville, N. C. Of these, roughly a dozen were possibly in progress at night (the precise occurrence times are not always listed) when RAE passed within about 1000 km of their location and, in addition, that location

was storm-free five nights earlier or later for control purposes.

Corresponding ionospheric critical frequency data were obtained from WDC, Boulder, Colorado for the stations Boulder, White Sands and Wallops Island to calibrate the CRPL median prediction maps in the vicinity of the storm region, and thereby gain an estimate of ionospheric shielding at the times of interest.

Variations in equivalent noise temperature generated by thunderstorms, background noise (and distant transmitters) on control nights, as well as the extent of ionospheric shielding all appear to present first-order complexities in the analysis. Only two of the apparently simpler events are therefore treated here. These are passes over storms in the middle U.S. on the nights of 15/16 September 1969 and 28/29 September 1969, and their respective control nights of 20/21 (5 days after) and 18/19 (10 days before) September. The basic satellite data are in the form illustrated in Figure 10.

Lacking ground-based radio noise measurements in the geographical region of interest, it is appropriate to deduce the equivalent ground noise temperature on the basis of the satellite temperature and critical frequency measurements through eqs.6 and 7A (Section 2). Although one could as easily assign values to T_g from CCI (1964) or other predictions (e.g. Horner, 1965) and compute an expected noise temperature at the satellite for comparison with the measurements, it is felt that interference effects would be more evident in the results obtained by the method chosen.

Thunderstorm activity was reported in Wisconsin, and in the 3-state area of Kansas, Oklahoma and Nebraska in the night of 15/16 September 1969, as illustrated in Figure 11. In this night RAE passed near these areas to the northwest and heading southwest at about 0420 UT (~2115 LT). Five nights later RAE passed over going in the same direction along the track labeled "Control Pass 1"; storm data listings indicated no activity on the control night.

The satellite antenna temperature data, recorded as 32 sec averages, were averaged over a period of 160 sec (5 readings) centered on 0420 UT on the storm night and on 0359:30 UT on the control night, to establish a representative effective temperature, T_s. Considering the ionosphere to be the limiting factor in the size of the viewing area, each frequency sees a different area, (the highest frequency covering the largest area), but all four frequencies can see the storms.

A more detailed view of the ionosphere effect is given in Figure 12. For later discussion the position of a high-powered transmitter located in northern China is noted. The critical frequency distribution along the great circle path from the transmitter to the sub-satellite point was derived from the CRPL predictions corrected over the U.S. by the foF2 measurements at Boulder, White Sands and Wallops Island. The path is 10,300 km long, and its apex reaches 85°N geographic latitude.

The maximum distance, L, from the sub-satellite point that a point source could be located and still be seen by RAE on each frequency was deduced from eq. 7 according to the foF2 distribution along the path. Line-of-sight ray paths from each of these point source locations are constructed to the satellite position (neg-

lecting refraction) in Figure 12. It is evident that the range of view for 3.9 MHz is smallest, and the viewing angle at the satellite widens with increasing frequency.

To a first approximation the ionosphere can be considered to be concentrically distributed in this example, so that $L \simeq R$ is the radius of the viewing area. Utilizing these (Fig.12) values of R in Eq. 6 along with measured values of T_s (averaged over 160 sec.) the value of average ground temperature T_g within the viewing area was deduced for each frequency. The results are plotted in Fig.13, but before proceeding to that, a word about interference is in order in connection with Fig.12.

The transmitter in northern China is 100 kw operating on a frequency inside the 200 khz bandwidth of 9.18 MHz. It is one of approximately 15 such transmitters listed in the World Frequency Listing of ITU*; all of which are located in China and Russia and are 10,000 km or more from central U.S. It is therefore, representative of a possible interfering transmitter. Utilizing Davie's (1965) techniques for manual ray tracing in conjunction with the situation depicted in Fig.12, we find that the only ray paths open to signals from the transmitter to the satellite (again neglecting refraction) are 6 1/2 and 7 1/2 hops. The total path distances are in excess of 10,000 km, at least the first three and a half hops are on the day side, the paths cross the auroral zone twice, and the two paths have three and four ground reflection points, respectively.

Assuming that the 100 kw transmitter is 10% efficient feeding a transmitting antenna with zero gain, and taking account of the transmission losses (i.e. distance antenuation, daytime absorption,

* International Telecommunication Union

auroral absorption and ground reflection loss), the computed received power converted to equivalent temperature in dB > T_o is 30 dB for 6 1/2 and 7 1/2 hops, respectively. These levels are more than 30 dB lower than the RAE measured temperatures. Further, since there are no transmitters operating on any of the assigned RAE frequencies in the U.S., a similar set of circumstances would prevail for those frequencies. It may be concluded, therefore, that for the events in question, the data are not contaminated by interfering transmissions.

Now returning to Fig. 13, along with the average source temperature at the ground deduced from the RAE measurements there are three prediction curves given. "JTAC" refers to the expected man-made noise level in an urban area as predicted by the Joint Technical Advisory Committee of IEEE (c.f., Herman, 1970). "CCIR" is the predicted median atmospheric noise level in the storm area (central U.S.) for 20-24 LT time block, summer season (CCIR, 1964). "Horner" is the average noise temperature required (on the ground in a thunderstorm area with radius 1000 km) to give the power flux density predicted by Horner (1965) for an altitude of 1000 km.

The source temperatures deduced from RAE measurements and the elementary theory embodied in Eqs. 6 and 7 are plotted in Fig.13 where the solid circles refer to the storm data of 16 September 1969, and the open circles are the corresponding control day of 21 September. The solid blocks are for a second storm observed over Minnesota on 29 September 1969, with corresponding control day data (open blocks) on 19 September (no data were available 5 days before or after the 29th).

As it turned out, on both control nights the critical frequency over the storm area was greater than 4.7 MHz, so we have no control data on the lower frequencies.

Comparing the storm nights, the September 16 storm apparently covered a larger geographic area than the Minnesota storm judging from the WDC storm data reports, and the measured temperature (solid circles) on the 16th is about 4 dB higher than on the 29th (solid blocks) on all four frequencies. The frequency dependence for both storms is consistent with that expected from thunderstorm noise. Both storm passes see temperatures 4 to 8 dB higher than the noise level expected in urban areas. Compared to the control nights, the storm passes are 1 to 6 dB higher.

Briefly recapitualating the salient features of thunderstorm observation by RAE, the following factors should be emphasized:

1. The periods of observation are somewhat limited due to the constraint that the critical frequency distribution over the satellite viewing area be either circular or uniform in nature.
2. All of the storms investigated to date clearly display higher noise temperatures than is the case on "control" days, across the whole RAE Lower Vee Spectrum.
3. The size and intensity of an individual thunderstorm cannot be adequately determined utilizing present analytical techniques. However, it is believed that with a further refinement and sophistication of analytical techniques, size and intensity information can be extracted from the raw data.
4. Over the United States, the noise level appears to be quite high regardless of season (section 5), which implies a substantial background due to man made sources (not transmitters). When a thunderstorm does occur, it may

occupy only a fraction (perhaps 20-30%) of the total area observable by the satellite. The conversion technique utilized in this analysis forces the equivalent ground temperature to be the average temperature over the whole viewing area, which would be considerably less than the temperature of the thunderstorm. This average ground temperature, when compared to the already high background noise level from man made sources, is only about 5 dB greater in the cases investigated. It is expected that, in regions where the background level is low, such as over the oceans, the storm-time level can be quite high in comparison. In section 5, a case of this nature is investigated.

5.0 Noise Contour Mapping

5.1 Preparation of Maps

Contour maps of terrestrial noise distributions have been generated manually in the manner described by Herman and Caruso (1971). Selection of the data was restricted to periods in 1968 and 1969 when RAE was nominally over Earth's night side. For 1968 data, in the local time block periods of 20-24LT, 00-04LT and 04-08LT, the ephemeris information printed out at 15-minute UT intervals was manually searched to find local times falling into the above LT time blocks. Usually only 2 points within a block were found. At these points the universal time and geographic location of the satellite were noted, and the noise magnitude at that UT time was extracted from the whole-orbit RV data tabulated on microfilm and converted to decibels (dB) above 288^{o}K. On base maps cast in modified-cylindrical (geographic) coordinates each noise magnitude was recorded at its appropriate location, and then isolines of constant noise level in 5-dB increments were drawn manually through the data points. Data from consecutive passes covering approximately five days were required to obtain full longitudinal coverage of the globe. For 1969, the available ephemeris is listed at 10-minute intervals, increasing the number of data points by about 50%.

The first global map of terrestrial radio noise prepared earlier in this manner, based on RAE data taken on 9.18 MHz in December, 1968, is in publication (Herman, et al, 1973), and is reproduced here in Figure 14 for comparison with additional maps generated under the present contract. For the December, 1968, period, data on the frequencies of 6.55, 4.7, and 3.93 MHz were mapped in like manner. The ionosphere

was opaque to 3.93 MHz terrestrial noise over most of the global surface, but useful maps for 6.55 and 4.7 MHz were obtained. These are given in Figs.15 and 16. These maps exhibit frequency variations of distributions obtained in a single time period. To illustrate variations with month, maps of 9.18 MHz noise for October, 1968, and August, 1969, are given in Figs. 17 and 18.

5.2 Spatial Distribution Variation with Frequency

In considering the December series (Figs. 14-16), it is evident that there are a number of similarities between frequencies, but also some differences. As a generality, it can be said that the regions of high noise activity in the northern hemisphere on all three frequencies are centered over the continental land masses, and the magnitudes are higher over Eastern Europe and the Far East than over North America. Further, the noise level is lower over the northern oceans than over the land masses. Note that over the North Atlantic Ocean, the magnitude on 9.18 MHz is ~60-65 dB, on 6.55 MHz, it is ~55-60 dB, and on 4.7 MHz, about 45-50 dB.

Over Europe and the Far East, the geographic region contained within the, say, 65-dB contour shrinks successively in going from 9.18 MHz through 6.55 to 4.7 MHz (Figs.14, 15, and 16, respectively).

In the southern hemisphere, where the measurements were in summer and mostly in the local time period 00-04LT, the ionospheric critical frequencies were generally higher than in the (winter) northern hemisphere, where the time of observation was 04-08LT corresponding to the predawn minimum in critical frequency. Thus, the RAE observing

frequency of 4.7 MHz was always less than foF2 in latitudes from 0° southward (southward of about 20°S over South America), and the noise level depicted in Fig.16 below the equator corresponds to the cosmic noise background. To some extent, the higher critical frequencies also affect the 6.55 MHz distribution (Fig.15). Compare, for example, the contours over South America with those of 9.18 MHz (Fig.14).

An interesting small feature appears at about 5°N, 170°W on both 9.18 and 6.55 MHz, but a corresponding maximum was not seen here on 4.7 MHz. It is probably due to an ocean thunderstorm, since it was observed on both of the higher frequencies, but the ionospheric opacity precluded observation on 4.7 MHz. This feature contrasts to a similar one observed at about 38°N, 170°W on 6.55 MHz only; a maximum occurring on a single frequency such as this is more likely due to detection of a ground-based transmission.

In still another case, the small isolated high on 6.55 MHz at 15°N, 60°W is probably connected to the top of the South American high due to thunderstorm activity seen on 9.18 MHz (Herman et al, 1973), but ionospheric cutoff obscures most of that region on the lower frequency map. Such an argument, that is ionospheric cutoff, is further supported by the lack of any corresponding feature on the lowest frequency (4.7 MHz) map in Fig.16.

Other localized features observable in the maps must be analyzed on an individual basis, too, because of the continuing interplay between source types on the ground and variations (both spatial and temporal) in the intervening ionosphere. The important point to remember is that, in spite of any difficulties in interpreting specific

features, these maps represent the noise distributions as seen by the RAE satellite on 9.18, 6.55 and 4.7 MHz in the period 00-08LT, December 2-6, 1968. With the exception of modifications that would be imposed by a different bandwidth, and possibly by a different antenna configuration, they represent the distributions which would have been seen by any other satellite in the same orbit during that period. As we have seen, the ionosphere imposes a greater restriction on the character of the terrestrial noise component on frequencies of 3.9 to 9.18 MHz at satellite altitude than does the receiving antenna pattern.

5.3 Month-to-Month Variations

Major features of the 9.18 MHz December map (Fig.14) have already been discussed in the previous section and by Herman, et al (1973). Emphasis here will, therefore, be on the October, 1968, and August, 1969, maps for 9.18 MHz (Figs. 17 and 18).

In October, RAE was over the southern hemisphere in the period 00-04LT, and over the northern hemisphere between 04 and 08LT. It crossed the equator close to 04 LT on each pass, and again, approximately five days were required to obtain full 360^{o} longitudinal coverage in the time period 00-08LT.

According to the ionospheric predictions (ESSA, 1968), at 04LT the highest critical frequency should not have been greater than about 7 MHz at all longitudes, so the ionosphere should have been transparent to 9.18 MHz while RAE was over the equatorial latitudes. At the beginning (00LT) and end (08LT) of the period of interest, the low latitudes had critical frequencies of 9.2MHz or greater, as illustrated in Fig.19. However, at hours close to 00LT

was generally in high southern latitudes and, therefore, outside of the region where foF2$\geq$ 9.2 MHz, and as the satellite moved equatorward it encountered times near 04LT where foF2 was still < 9.2 MHz. In the northern hemisphere the local time at the satellite progressed toward 08LT as RAE moved northward, so that it was nearly always north of the region of foF2$\geq$ 9.2 MHz. (See Fig. 19).

Thus, consideration of predicted critical frequencies shows that for the October, 1968, 00-08LT period, the critical frequency of the ionosphere directly below the satellite was practically always less than the observing frequency of 9.18 MHz. Variations in the noise distribution presented in Fig.17, therefore, reflects primarily the source distribution rather than the critical frequency distribution. The size of the ionospheric iris (Section 2.1) will, of course, affect the absolute magnitude of the observed noise, so the contours at altitude do not necessarily represent the undistorted noise source distribution.

Neglecting possible distortions introduced by the iris, however, it can be seen in Fig.17 that, as in December, the October noise level is highest over the continental land masses and lowest over the ocean areas far removed from land. In going southward from the equator, the noise level exhibits a gradual decrease toward the higher latitudes in spite of the fact that the iris is growing bigger due to decreasing critical frequencies.

The August, 1969, distribution for 9.18 MHz (Fig.18)was constructed a bit differently from the October and December maps. Firstly, it is based on a higher point density afforded by the 1969

ephemeris data plus 20 days of observational data rather than five days. Secondly, to achieve full latitudinal coverage it was necessary to accept local times in the period 04-12LT rather than 00-08LT. No data were available in the northern hemisphere of the Far East due to malfunction of an on-board tape recorder. During August the orbit of RAE was such that the satellite was over high northern latitudes ($> 55^{o}N$) near 04LT, and as its position progressed southward the local time increased, being near the equator at 08LT and $>50^{o}S$ at 12LT. (Fig.20).

This progression of local time allows mapping of the August noise with minimum interference from the ionosphere, but as will be seen, complete opacity for 9.18 MHz was encountered over a portion of the orbits. At 04LT and 06LT the critical frequency was always less than 6.2 MHz at all predicted longitudes, and at 12LT the predicted foF2 was less than 9.2 MHz at southern latitudes greater than about $18^{o}S$, as illustrated in Fig.20.

When RAE was in the vicinity of the equator at 08LT, the geographic region containing foF2 $\geq$ 9.2 MHz and $\geq$ 6.2 MHz was as depicted in Fig. 21, a local time (08LT) critical frequency map extracted from the ESSA (1968) predictions. One can imagine a dynam. picture wherein the satellite is over an ionosphere whose critical frequency is always >9.2 MHz as it travels southward in the northern hemisphere, encounters the newly developing region of high foF (>9.2 MHz) near the equator when the local time is ~08LT, and then stays well ahead of the expanding opaque ionospheric region in its still southward journey below the equator from 08LT to 12LT. A typical example of this progression is given in Fig. 20, where the

critical frequencies as a function of latitude and local time at 75°E are superimposed on the RAE track.

With this picture in mind, the noise contour map in Fig. 18 for 9.18 MHz in August, 1969, may be examined. Again in this month it is to be noted that, just as in December and October, the prominent regions of high noise levels are over the continental land masses and the low regions are over the oceans. The effect of ionospheric shielding is clearly evident in the latitudinally narrow region of high foF2($\geq$9.2 MHz) extending across the map near the equator. Within the bounds of this region(reproduced by dashed lines in Fig.18) the noise level is 50 dB or less, and it is to be noted that over South America where the shielding region temporarily disappears the noise level increases to 60 dB and more. The correspondence between high foF2 and low noise is not perfect in this map (Fig.18);e.g.,the 60dB contour at 5°N, 135°E and the one over equatorial Africa are in the opaque region. However, it must be remembered that the ionospheric prediction is for median conditions in August, and the opaque region would be smaller or nonexistent on 50% of the days. Both north and south of this region foF2<9.2 MHz, so the noise contours represent primarily source changes.

An area of potentially great significance appears in the Indian Ocean between Madagascar and Australia, bounded roughly by latitudes 20 - 40 ° S and longitudes 60-105° E.(Fig.18). Here there are clearly localized regions of high noise level (70dB) imbedded in an area where the ambient was more like 50dB. The expected critical frequency in this area, as evident in Fig.20, was less

than the observing frequency of 9.18 MHz and greater than 6.55 MHz. These localized highs were encountered on five separate pass dates (Aug. 8, 18, 20 ,25, 26) out of the total of 20 days utilized for the map, and on the remaining days the noise level in this region varied from about 50 to 55 dB.

Unlike the thunderstorm passes over the U.S. analyzed in Section 4 , the background noise level in the Indian Ocean is quite low due to the absence of man-made sources, so an active thunderstorm would raise the observed noise level considerably above background. It thus appears that the high noise area observed over the Indian Ocean stems from ocean thunderstorm activity. We believe this to be an unusual occurrence considering that, in addition to it being over an ocean where few thunderstorms are generally thought to occur, it is also in local winter, a season of low thunderstorm activity. Because the critical frequency in August was too high, this unusual region was not detected by RAE on the observing frequencies below 9.18 MHz. An isolated high of 65 dB was observed in the same Indian Ocean area in October (spring) on 9.18 MHz (Fig. 17), but not in winter (December, Fig. 14).

In all three months (Figs. 14, 17, 18) the U.S. is covered by a high region of 60-65 dB lending support to the earlier conclusion (Herman, et al, 1973) that the principal terrestrial component here is due to man made sources. Northern China, Russia and the eastern Mediterranean areas are covered by highs of 70-75 dB in October and August as well as in December, and this constancy further supports also the earlier conclusion (Herman, et al, 1973) that in these areas, commercial transmitters operating within the bandwidth of the 9.18 MHz frequency are the major contributors.

Over northern South America, where thunderstorm activity is believed to be the major contributor (Herman, et al, 1973), the highest levels observed were 75 dB (or greater) in December, 65 dB in October and 70 dB in August. As RAE passed over the middle of this region (0°, 60°W) in December and October, the predicted critical frequency was 4.2 MHz for both months, and for August it was 7.8 MHz. The nominal size of the iris was thus about the same in December and October, yet the observed October noise magnitude was about 10 dB lower than it was for the December passes, implying less thunderstorm activity in the October period. In August the nominal iris was smaller than in the other two months, so the source strength must have been considerably larger than in October, and perhaps greater than in December.

6.0 Summary and Conclusions

Results of our continuing investigation of radio noise received by the Radio Astronomy Explorer satellite on its downward looking Vee antenna further strengthen the conclusion that terrestrial radio noise penetrating through the ionosphere on Earth's night side and other regions where the critical frequency is low produces at 6000 km altitude a noise environment which is up to 50 dB or more higher than cosmic noise background.

A first-order theoretical treatment taking into account ionospheric shielding, extended source of noise from the ground and antenna configuration has yielded a working relationship between antenna temperature measured at the satellite and the equivalent average source temperature at the ground. That is, based on flat earth geometry,

$$T_s = \frac{1}{2} T_g G_s \log_e \left(\frac{R^2+H^2}{H^2}\right)$$

Where T_s is the satellite antenna temperature at altitude H, and T_g is the average noise temperature which would be measured by an omnidirectional antenna placed on the surface at a point within the effective circular source area of radius R. (G_s is the satellite antenna power gain.)

For an ionosphere with a critical frequency of f_c and layer maximum height of 300 km, spherical earth and satellite height of 5850 km, the effective ground range, L, from source to subsatellite point is given by (Herman, et al, 1973)

$$\frac{f_c}{f} = \left[1 - \frac{\sin^2 (L/R_e)}{1.39-1.14 \cos (L/R_e)}\right]^{1/2} \quad (7)$$

Where f is the observing frequency and Re is radius of Earth (6370 km). The constants are a function of layer height and satellite height.

With a flat-earth approximation and an ionosphere whose critical frequency is constant or circularly concentric over the effective source area,

$$L \approx R$$

Except when ground-based transmissions interfere on a specific frequency, the noise temperature due to terrestrial sources measured by RAE increases with increasing observing frequency, even though atmospheric and man made radio noise both have an inverse frequency dependence. Our simplified theoretical model shows that the increase at altitude is due to the expanding effective source area seen by the antenna at higher frequencies. This increase in source size overrides the decrease in intensity per unit area.

For a selection of passes over the central Atlantic and northern Pacific Oceans, the surface noise temperatures deduced from RAE observations on the frequencies of 3.93 to 9.18 MHz agree with the slope but not the magnitude of noise curves predicted by CCIR (1964). In the cases investigated, the measured noise was about 15 dB higher than predicted, and it is tentatively concluded that the predicted values for those ocean locations were too low.

Analysis has been made of passes over Pretoria, South Africa and Cook, Australia, where ground-based noise measuring stations and ionospheric sounders provide correlative data. Good agreement

was found between RAE noise expressed as equivalent source temperature and ARN-2 ground-based noise measurements.

The pass over Pretoria also offered opportunity to investigate quantitatively the effect of commercial transmitters located within the viewing area dictated by the ionospheric iris. It was found that the transmitted signal on 3.93 MHz saturated the receiver when RAE was north of the station, but as the satellite passed directly over the transmitter, the RAE antenna temperature dropped to a value consistent with the level expected from natural sources as measured at the ground by ARN-2. Measurements on 9.18 MHz on other passes over Urumschi, China where a high powered transmitter is located exhibit a similar behavior, that is, the noise magnitude is substantially lower when RAE is directly over the transmitter location. It is concluded that this behavior is due to the deep null in the vertical direction that is characteristic in the antenna patterns of transmitting antennas used by commercial broadcasters.

Night time passes over the United States during local summer were utilized to investigate the contribution of action thunderstorms to the noise level measured by RAE. After taking into account the ionospheric iris based on measured critical frequency values, it was found that the RAE noise level was 1-6 dB higher on storm time passes than on control passes going over the same region at about the same local time on nights with no reported storms. The RAE measurements on both storm and control nights rang from about 4 to 8 dB higher than the man made noise level predicted for urban areas. Local winter RAE data gathered in the period 00-08LT over the U.S., when converted to equivalent surface

temperatures using predicted critical frequency values exhibit magnitudes comparable to the summer control results. It, therefore, appears that man made sources provide a more or less constant high average background level. Atmospheric noise from thunderstorms covering only a portion of the effective source area (i.e., the total surface area visible to RAE through the iris) would thus add a relatively small amount to the total noise temperature.

The noise level due to thunderstorms occurring in regions where the background noise level is normally low, such as in ocean areas, would therefore be expected to be much higher than background. An example of this has been found in the Indian Ocean as a feature of the August, 1969 global map of 9.18 MHz noise. The RAE antenna temperature for the (assumed) storm passes, uncorrected for iris effects, was about 70 dB above 288^{o}K, a magnitude which is comparable to those normally observed over the South American continent, and which is about 20 dB higher than the background noise level usually observed over the Indian Ocean.

Manual ray tracing was utilized to assess the possible effect of distant transmitters on noise magnitudes observed by RAE over the U.S., South Africa and Australia. It was found that the signal from a 100 kW transmitter located about 10,000 km from the subsatellite point would produce an equivalent RAE antenna temperature about 30 dB lower than those actually observed. It appears that propagation losses in that part of the ray path which is below the ionosphere between the transmitter and ionospheric penetration point reduces the signal compared to the total noise radiated by the effective source area below the satellite. Further, no direct

paths which would minimize propagation losses between a transmitter and RAE can be identified by the manual technique; our interim conclusion, therefore, must be that the terrestrial noise observed by RAE comes only from the source area below the satellite visible through the ionospheric iris. This conclusion is supported by the fact that visual inspection of data taken on the dayside where foF2 >observing frequency for an estimated 2000 passes always finds the noise temperature on the downward Vee antenna to be equal to or less than that on the upper Vee - this indicates that all of the noise is coming from the galaxy and cosmic noise albedo from the top of the reflecting ionosphere.

Manual mapping techniques have produced global maps in geographic coordinates for noise distributions in December, 1968, on 9.18, 6.55, and 4.7 MHz, and in October, 1968 and August, 1969 on 9.18 MHz. (Other maps covering April and July, 1969 have been prepared, but were not treated here due to insufficient analysis of the results at contracts' end.)

The main features common to all maps, regardless of month or frequency is that the noise level is consistently high over the continental land masses and generally low over ocean areas remote from land. The ionospheric iris effect is quite evident on a global basis; the general noise level is highest on the highest observing frequency which sees the largest effective source area.

Our earlier conclusions (Herman, et al, 1973) based on 9.18 MHz observations in December, 1968, are borne out by the August and October maps for the same frequency. That is, over the U.S. the major terrestrial contributor appears to be man made noise; over China, Russia and the eastern Mediterranean area ground-based trans-

mitters operating in the RAE bandwidth contribute most; and over northern South America thunderstorm activity is the principal terrestrial source.

One discovery of potentially significant importance emerged from the August 9 MHz map. In the Indian Ocean area bounded by roughly 20-40°S and 60-105°E high noise magnitudes (~70 dB) were detected on five days out of the 20-day period of analysis, while the background level established by measurements in the remaining fifteen days was about 50 dB. In the absence of ship transmissions (the maritime frequency band is well outside the RAE bandwidth) or aeronautical signals, the high noise level would be due to intense thunderstorm activity.

This occurrence is believed to be unusual because it was observed in local winter, when thunderstorm activity is minimum, and was over an ocean area where few thunderstorms are generally thought to occur.

7.0 REFERENCES

1. Broadcasting Stations Of The World, Part II, Amplitude Modulated Broadcasting Stations According to Frequency, U. S. Government Printing Office, 1971.

2. Caruso, J. A. , J. R. Herman, and R. G. Stone, URSI paper Presented at Combined Session, Washington, April, 1972a.

3. Caruso, J. A., J. R. Herman, and R. T. Disney, paper presented at Fall URSI Meeting, Williamsburg, Va., December, 1972b.

4. CCIR, CCIR Report 322, International Telecommunication Union, Geneva, Switzerland, 1964.

5. Crichlow, W. Q., R. C. Davis, R. T. Disney and M. W. Clark, Hourly Probability of Thunderstorm Occurrence, Institute for Telecommunication Sciences, OT/ITS RR12, Boulder, Colorado, 1971.

6. Davies, K., Ionospheric Radio Propagation, U. S. Government Printing Office, 1965.

7. Herman, J. R., Progress in Radio Science, 1966-1969 (Brown, Clarence and Rycroft, Eds.) International Scientific Radio Union, Brussells, Belgium, 1970.

8. Herman, J. R., J. A. Caruso, and R. G. Stone, Planet. Space Science, Vol. 21, 1973.

9. Herman, J. R., J. A. Caruso, and R. G. Stone, Paper Presented at Waldorf Conference, Office of Naval Research, Arlington, Va., September, 1972a.

10. Herman, J. R., J. A. Caruso, and R. G. Stone, paper presented at Annual Fall Meeting, AGU, San Francisco, Cal., December 1972b.

11. Horner, F., Planet. Space Science, Vol. 13, 1965.

12. International Frequency Registration Board, International Frequency list, vols. I and II, International Telecommunication Union, Geneva, Switzerland, 1963.

13. Pierce, E. T., Planetary Electrodynamics, Chapter V-1, Gordon Breach, New York, 1969.

List of Figures

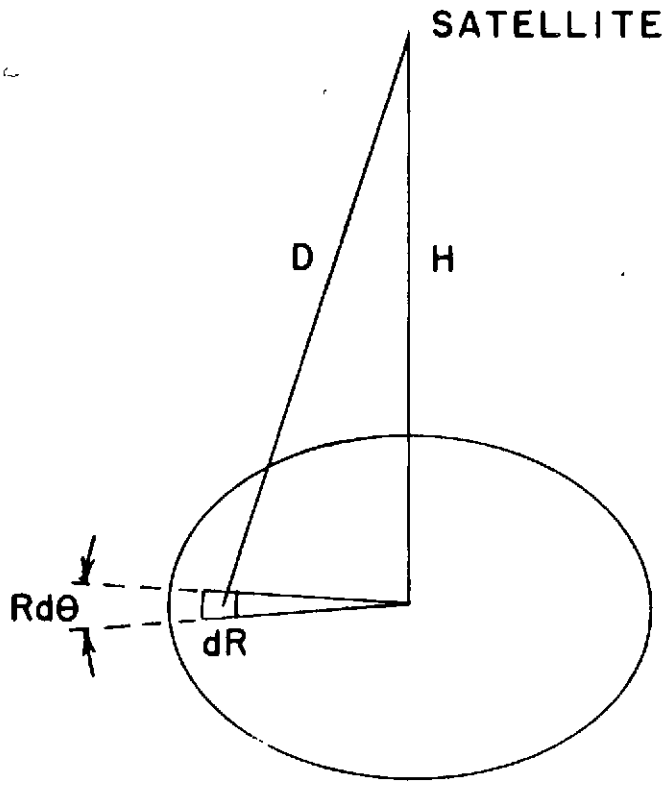

$$dP_s = \frac{Pg}{2\pi D^2} R d\theta \, dR$$

$$D^2 = R^2 + H^2$$

$$P_s = \tfrac{1}{2} P_g \ln \left(\frac{R^2 + H^2}{H^2} \right)$$

$$T_s = \tfrac{1}{2} T_g G_s \ln \left(\frac{R^2 \quad H^2}{H^2} \right)$$

FIGURE 1

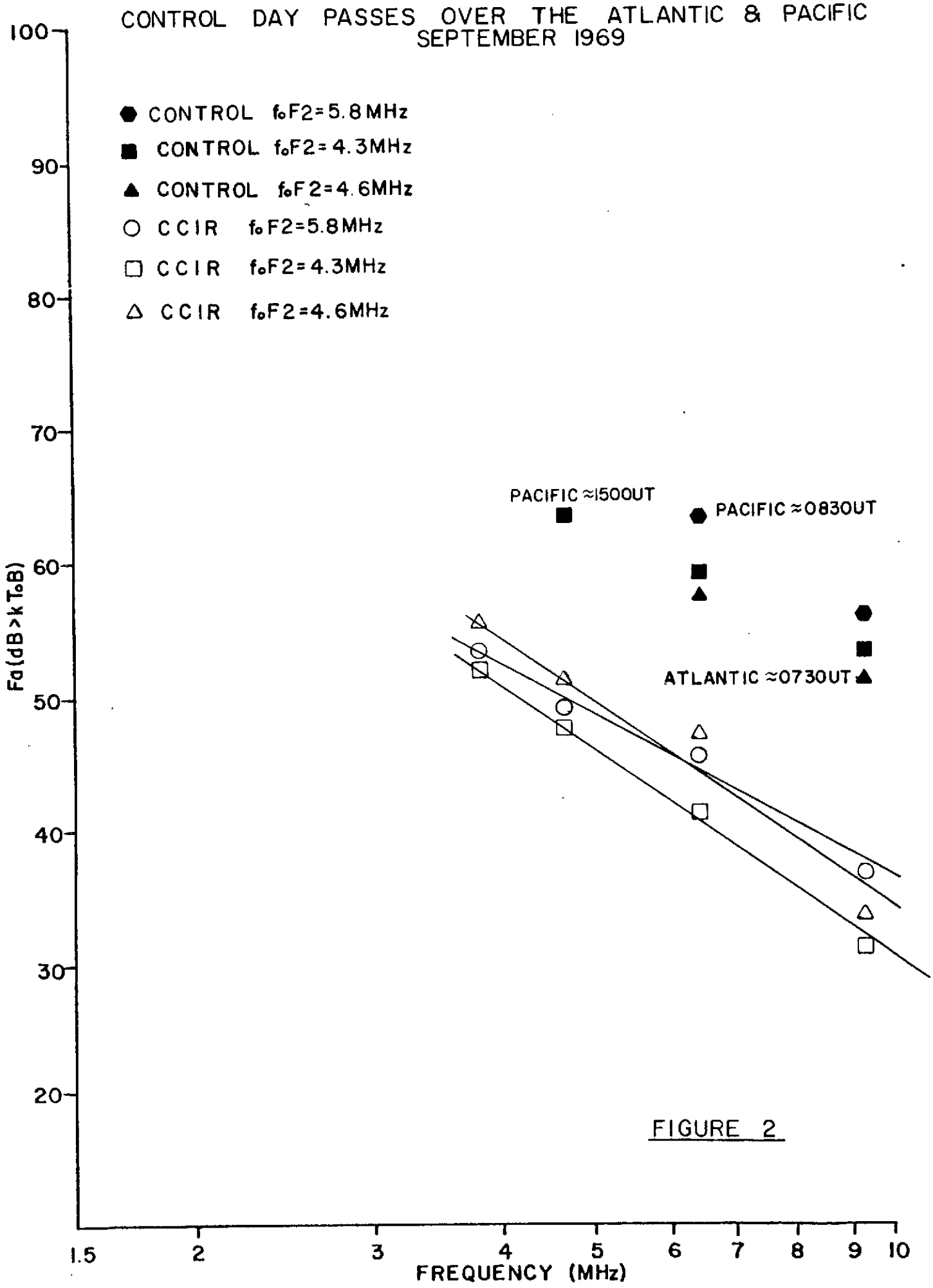
CONTROL DAY PASSES OVER THE ATLANTIC & PACIFIC
SEPTEMBER 1969
CONTROL foF2=5.8MHz
CONTROL foF2=4.3MHz
CONTROL foF2=4.6MHz
CCIR foF2=5.8MHz
CCIR foF2=4.3MHz
CCIR foF2=4.6MHz
PACIFIC ≈1500UT
PACIFIC ≈0830UT
ATLANTIC ≈0730UT
Fa(dB>kToB)
100
90
80
70
60
50
40
30
20
1.5
2
3
4
5
6
7
8
9
10
FREQUENCY (MHz)

FIGURE 2

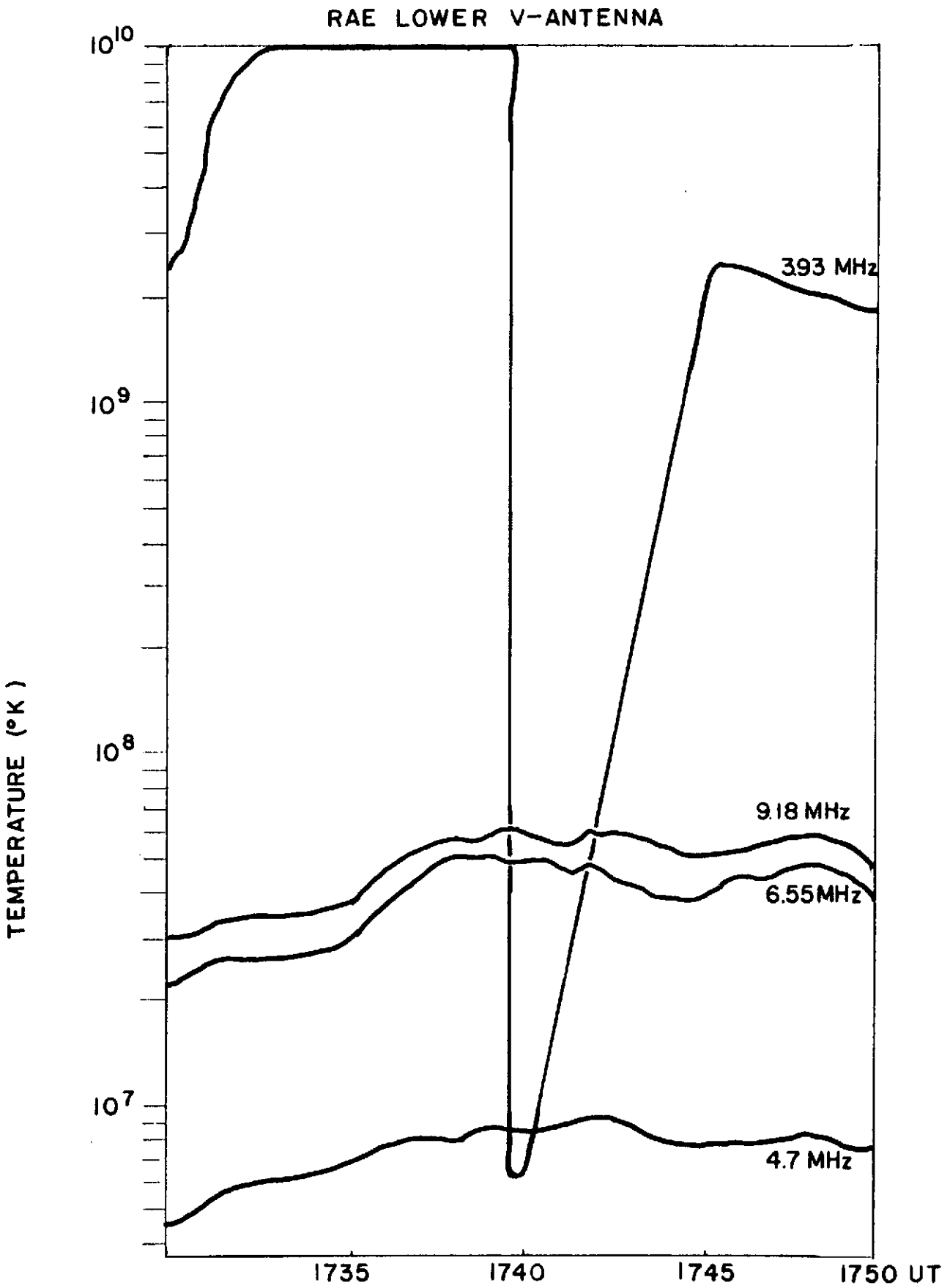
RAE LOWER V-ANTENNA
10^{10}
10^{9}
10^{8}
10^{7}
TEMPERATURE (°K)
3.93 MHz
9.18 MHz
6.55MHz
4.7 MHz
1735
1740
1745
1750 UT

FIGURE 3

RAE PASS OVER PRETORIA, SOUTH AFRICA
JULY 20, 1969

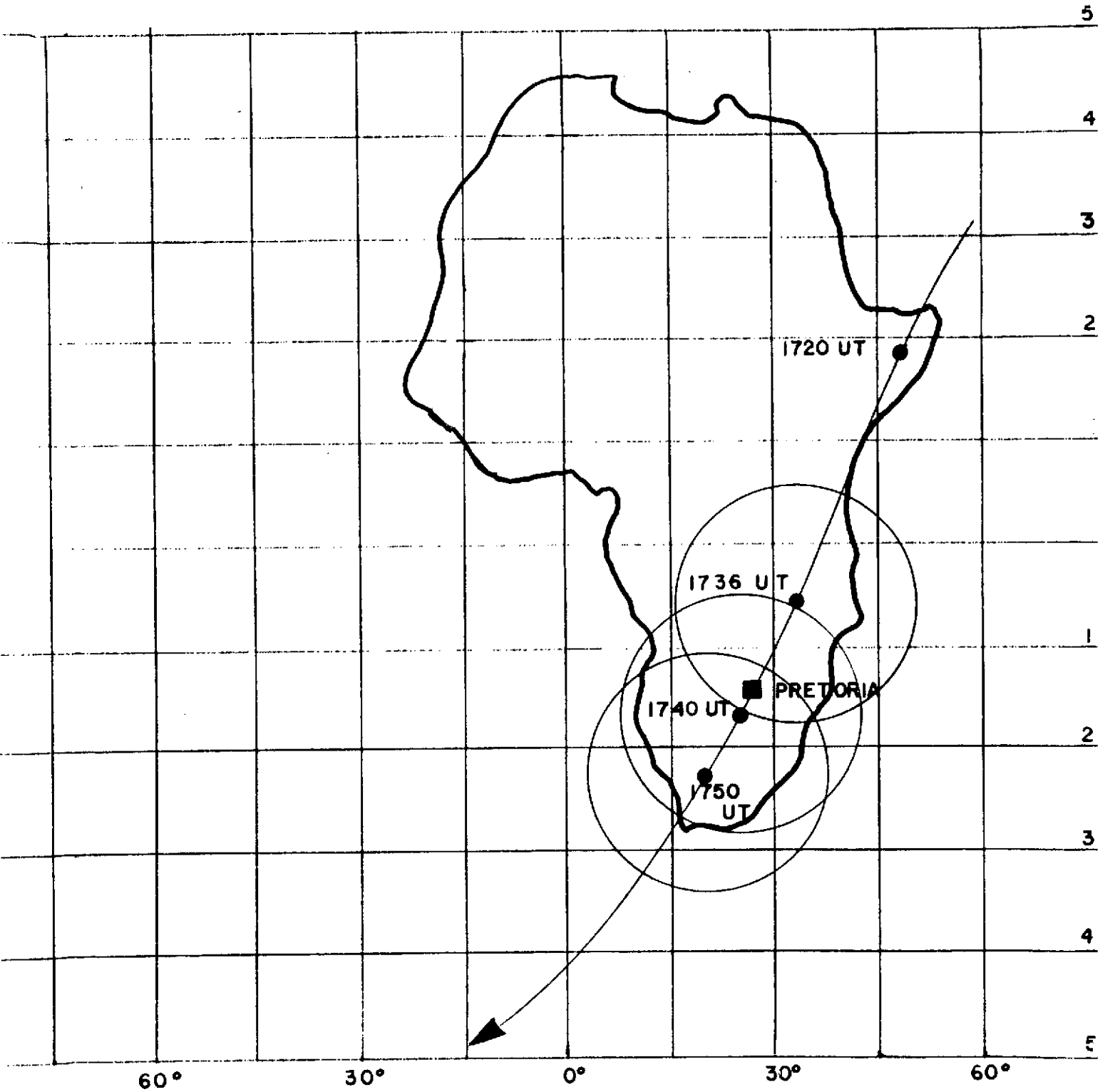

FIGURE 4

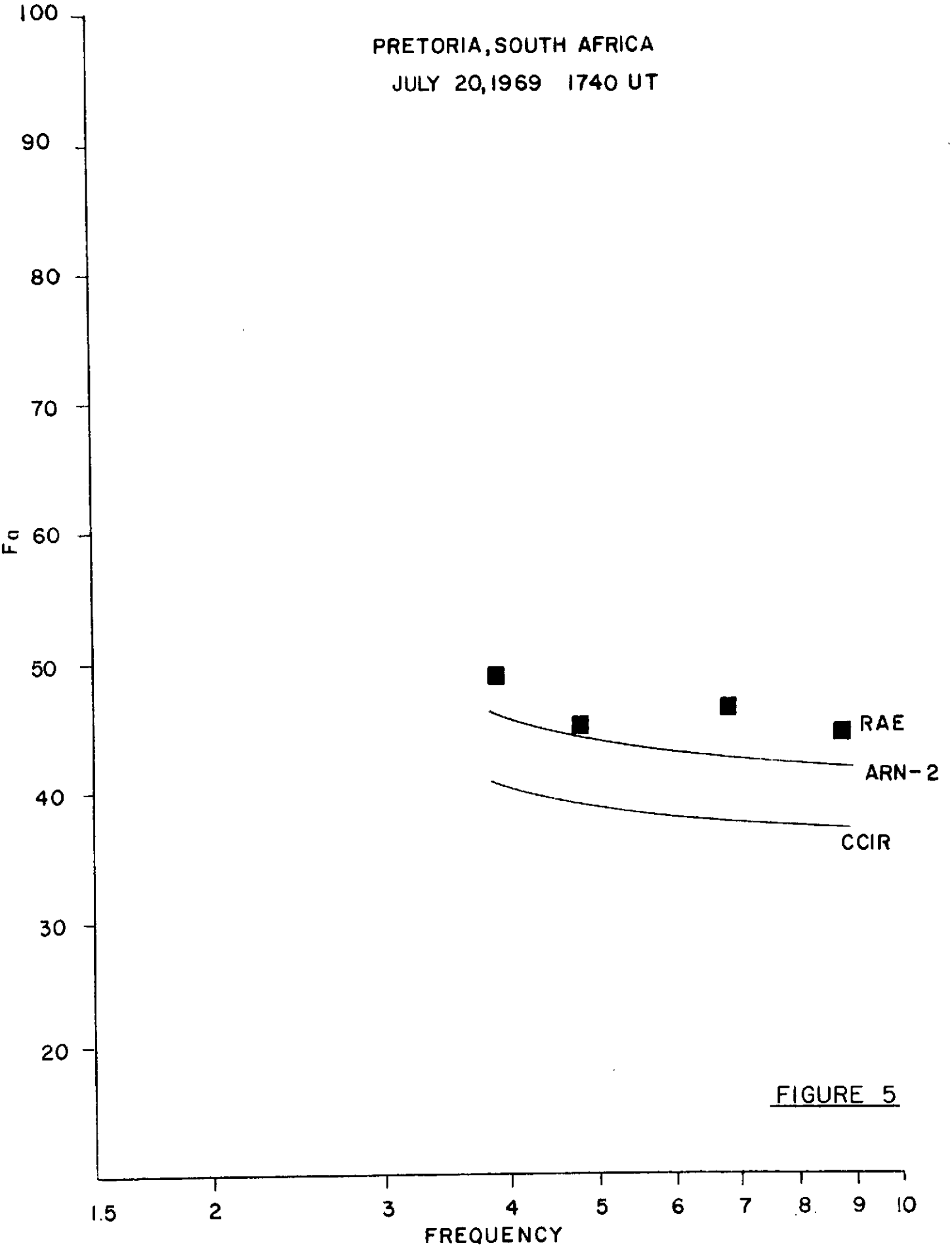
PRETORIA, SOUTH AFRICA
JULY 20, 1969 1740 UT
100
90
80
70
60
50
40
30
20
Fa
RAE
ARN-2
CCIR
1.5
2
3
4
5
6
7
8
9
10
FREQUENCY

FIGURE 5

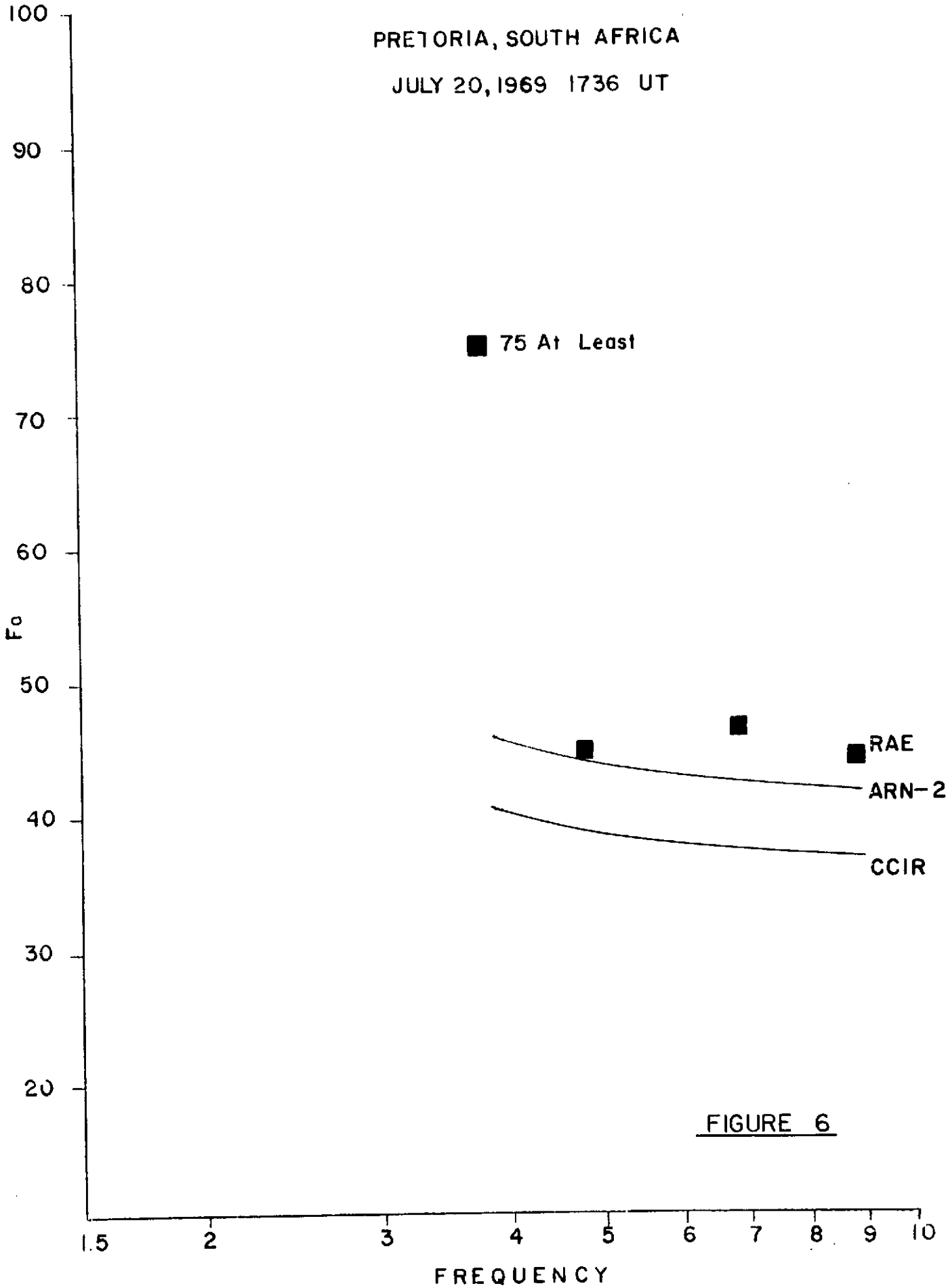
PRETORIA, SOUTH AFRICA
JULY 20, 1969 1736 UT
75 At Least
RAE
ARN-2
CCIR
Fo
100
90
80
70
60
50
40
30
20
1.5
2
3
4
5
6
7
8
9
10
FREQUENCY

FIGURE 6

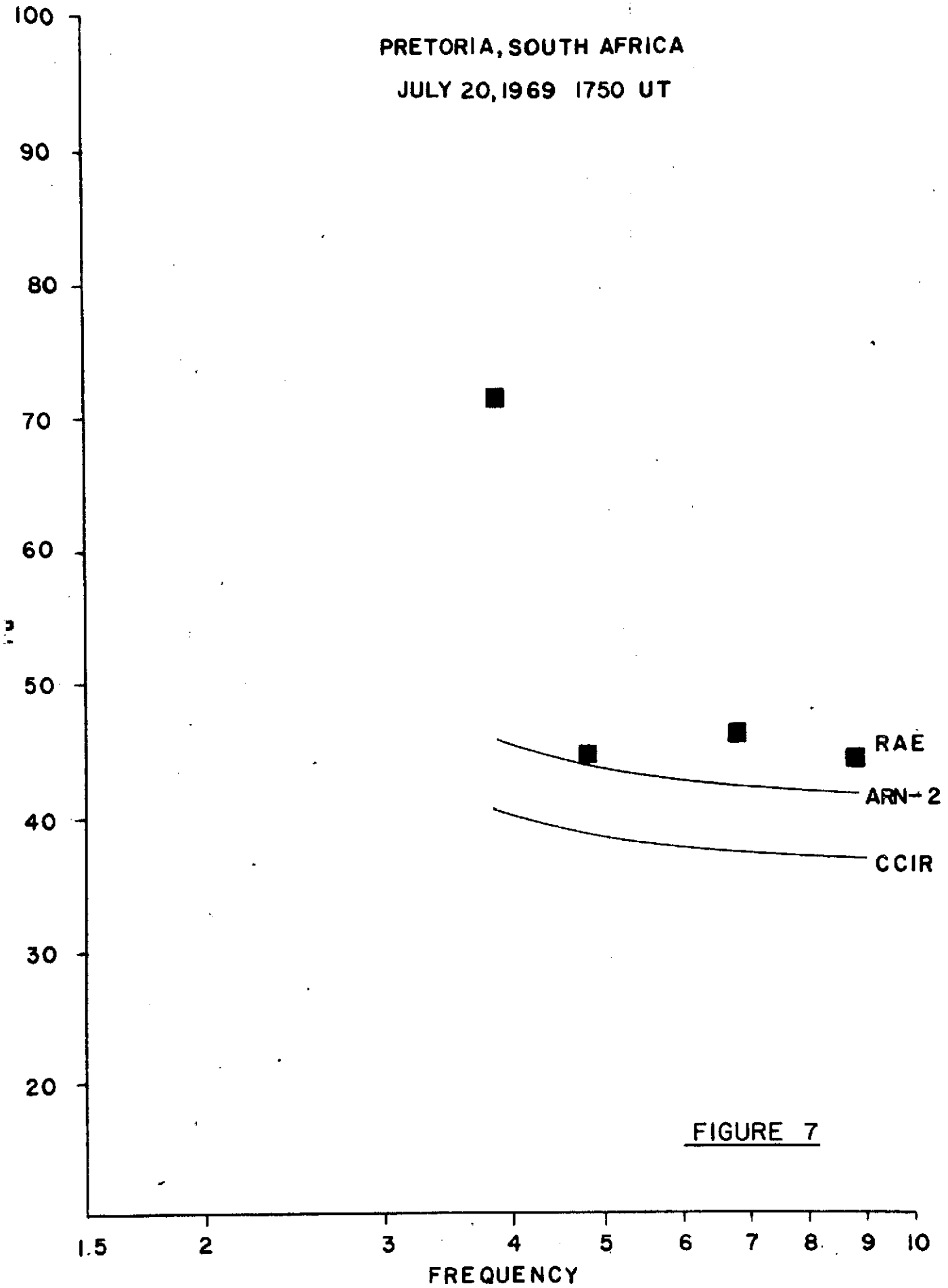
PRETORIA, SOUTH AFRICA
JULY 20, 1969 1750 UT
100
90
80
70
60
50
40
30
20
RAE
ARN-2
CCIR
1.5
2
3
4
5
6
7
8
9
10
FREQUENCY

FIGURE 7

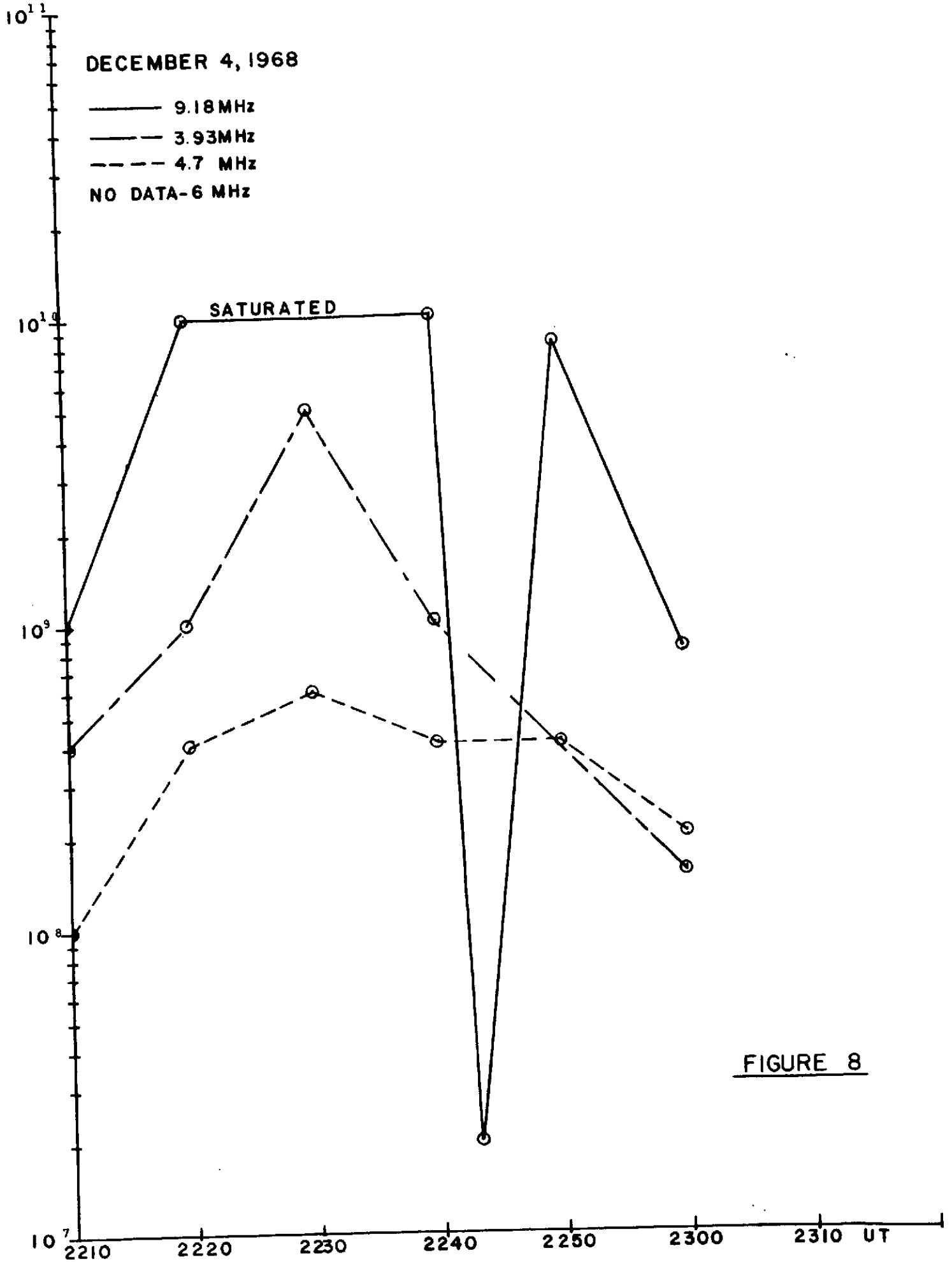
DECEMBER 4, 1968
9.18 MHz
3.93 MHz
4.7 MHz
NO DATA-6 MHz
SATURATED
10^{11}
10^{10}
10^{9}
10^{8}
10^{7}
2210
2220
2230
2240
2250
2300
2310 UT

FIGURE 8

JULY 20, 1969 1740 UT

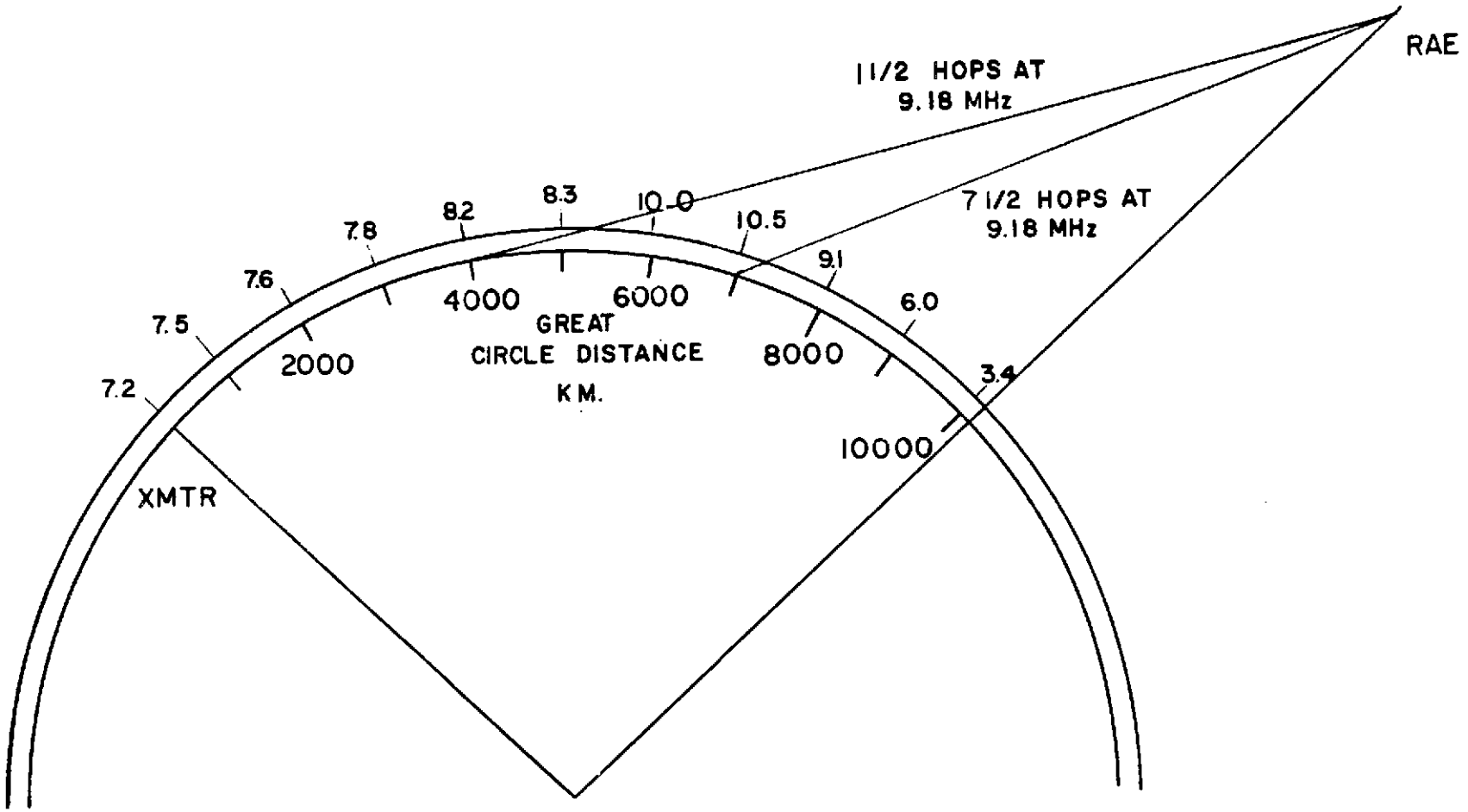

FIGURE 9

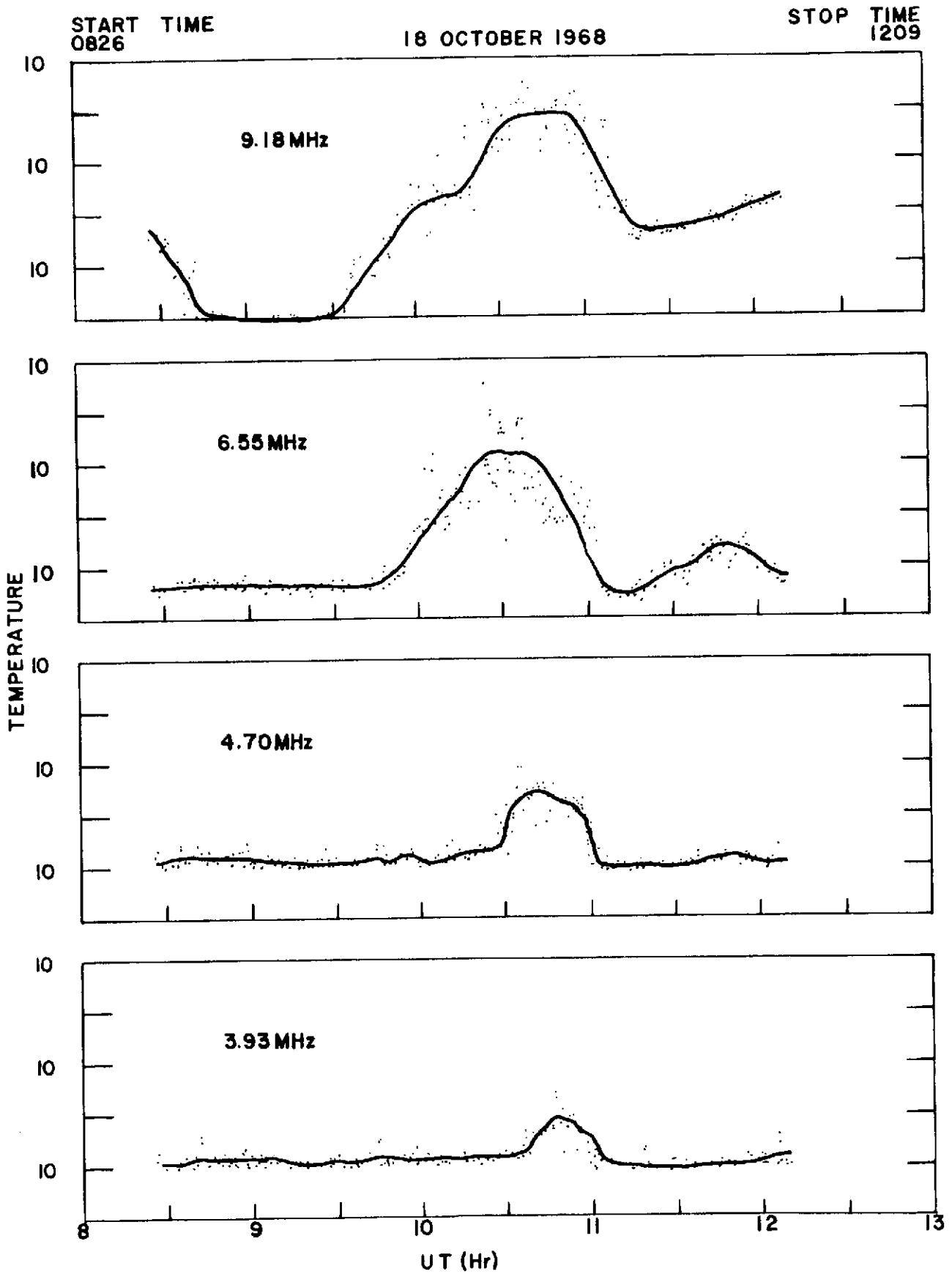
START TIME
0826
18 OCTOBER 1968
STOP TIME
1209
9.18 MHz
6.55 MHz
4.70 MHz
3.93 MHz
TEMPERATURE
10
UT (Hr)
8
9
10
11
12
13

FIGURE 10

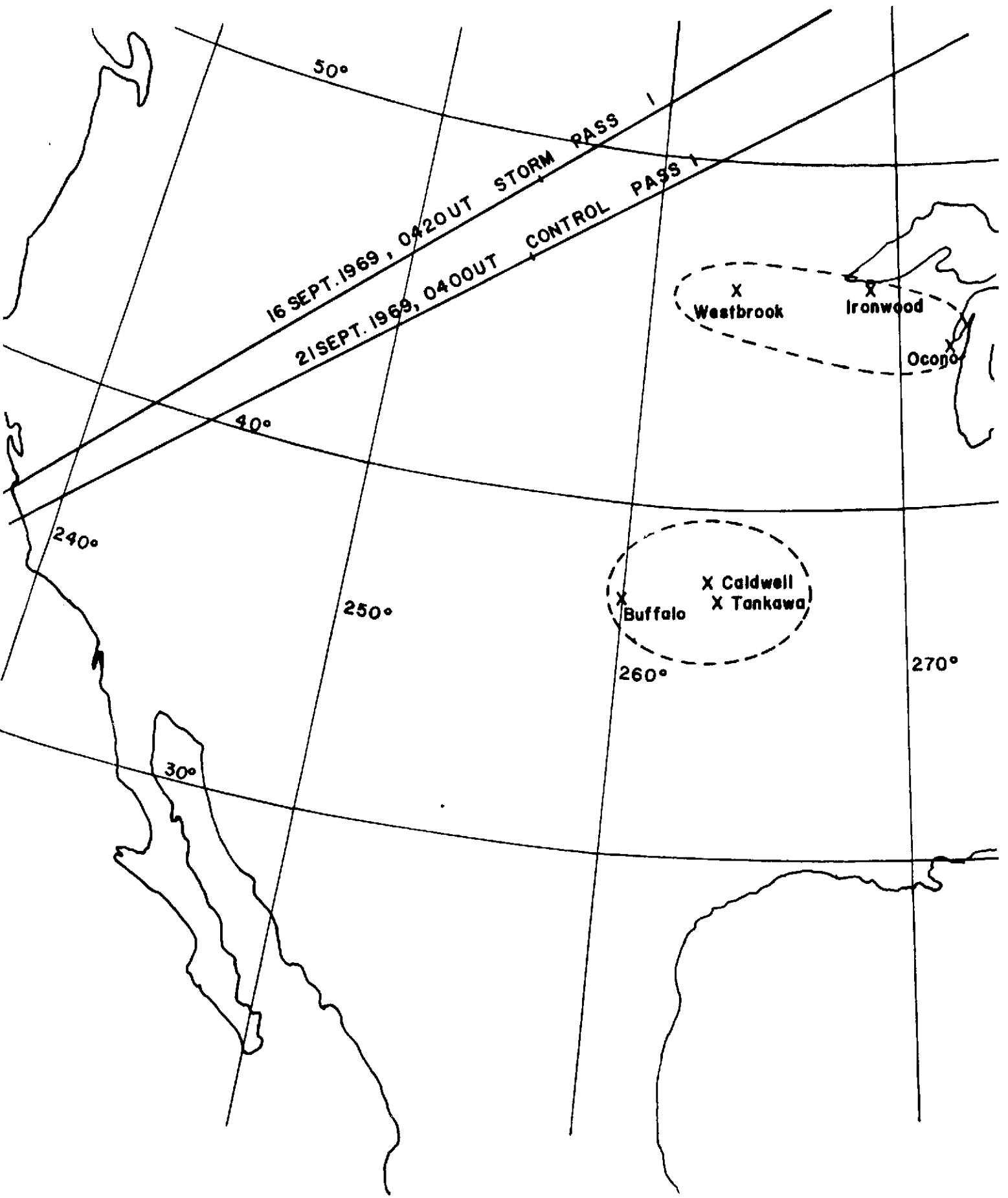
50°
16 SEPT. 1969, 0420UT STORM PASS 1
21SEPT. 1969, 0400UT CONTROL PASS 1
Westbrook
Ironwood
Ocono
40°
240°
250°
Buffalo
Caldwell
Tankawa
260°
270°
30°

FIGURE 1

16 SEPT 1969, 0400 UT

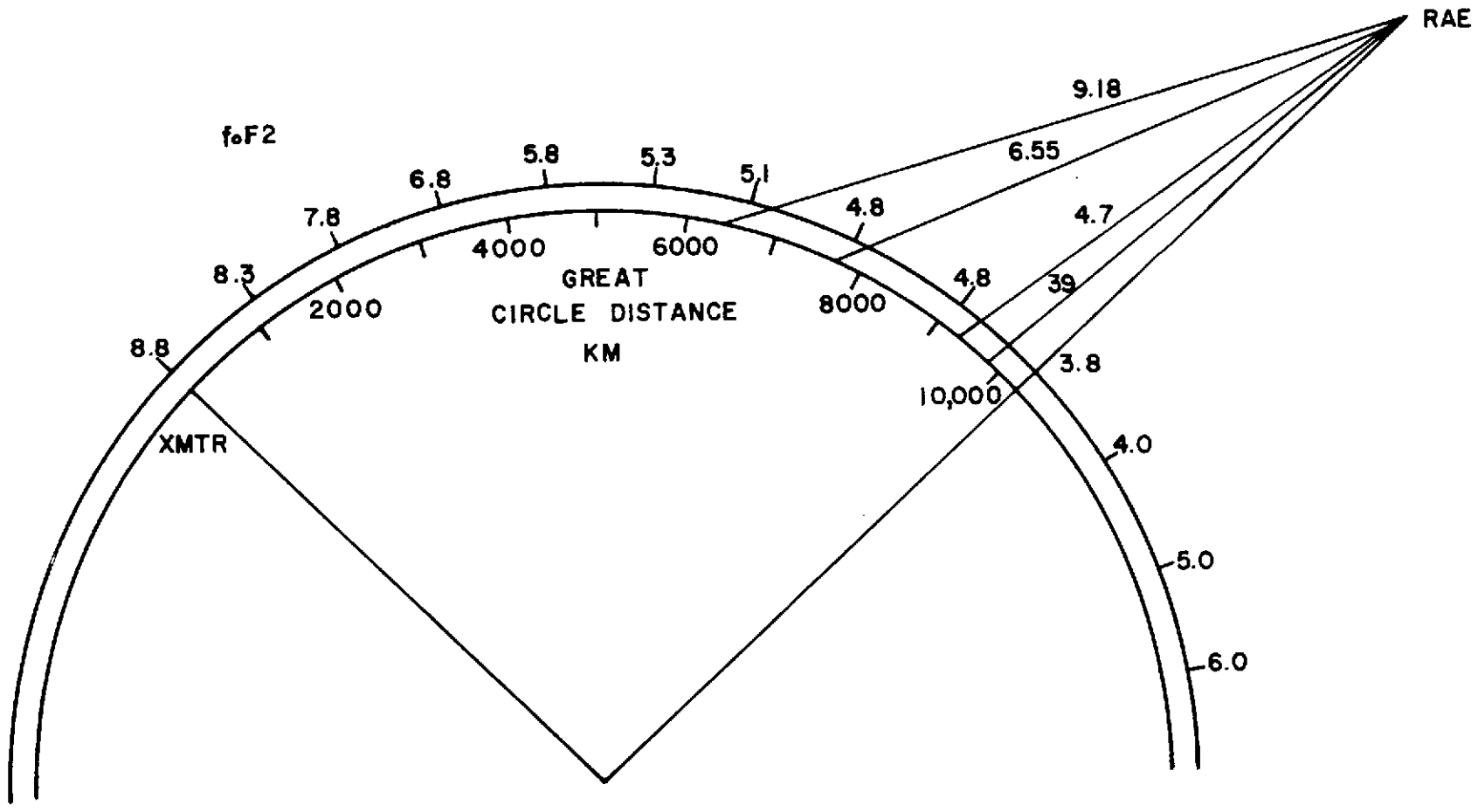

F
RE 12

05

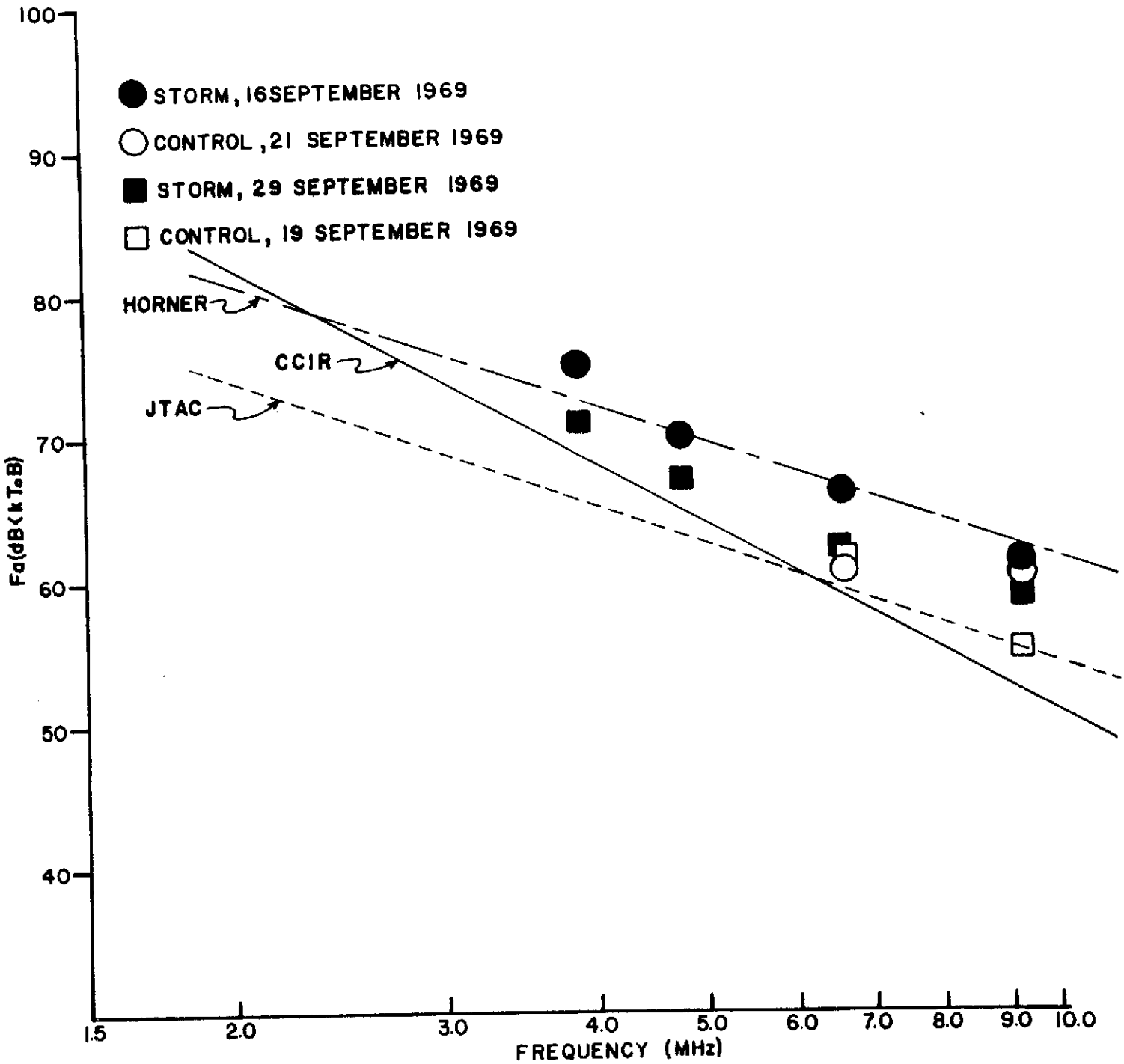

FIGURE 13 RAE I OBSERVATIONS OF THUNDERSTORMS OVER WISCONSIN AND MINNESOTA

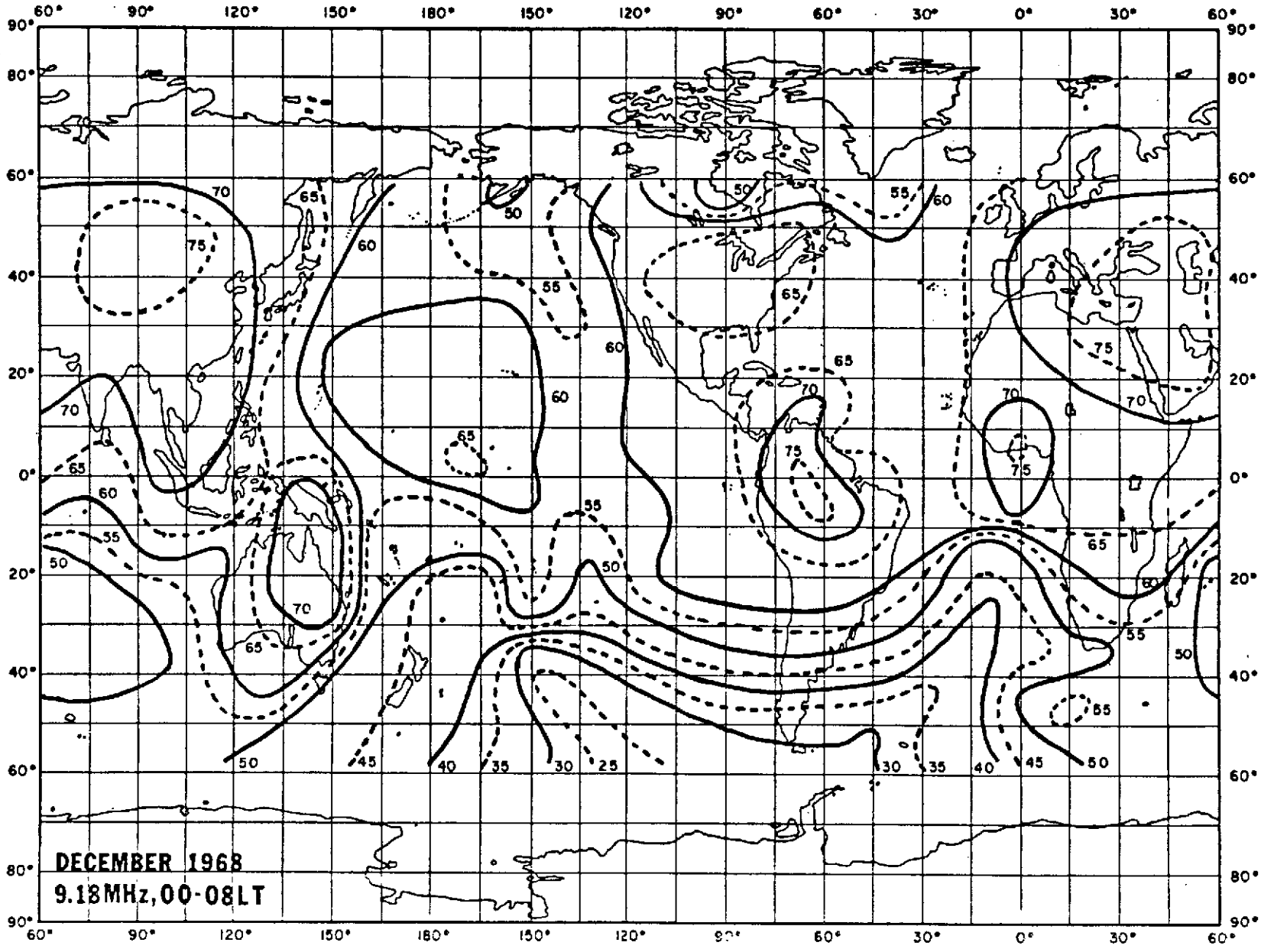

FIGURE 14

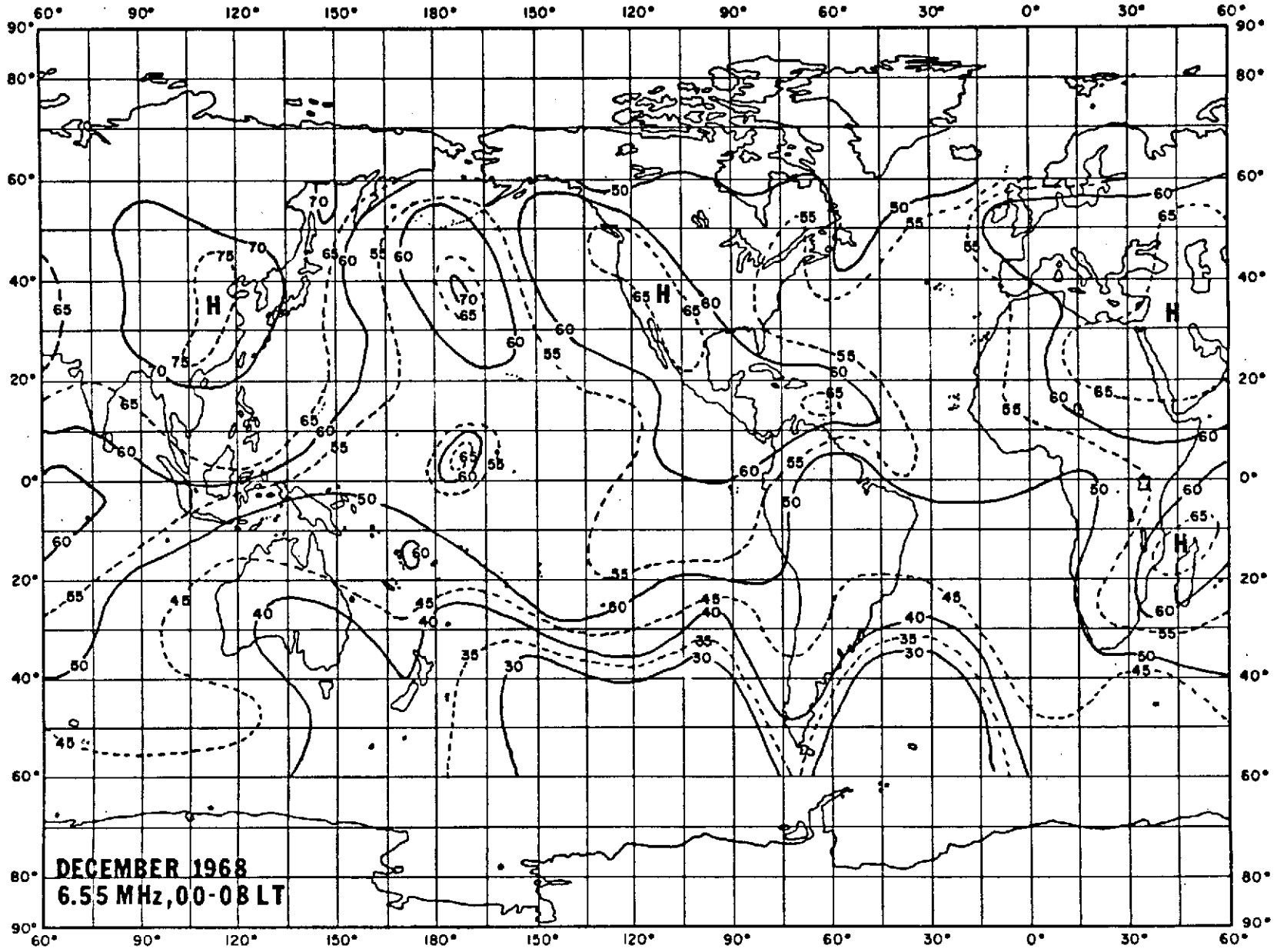

FIGURE 15

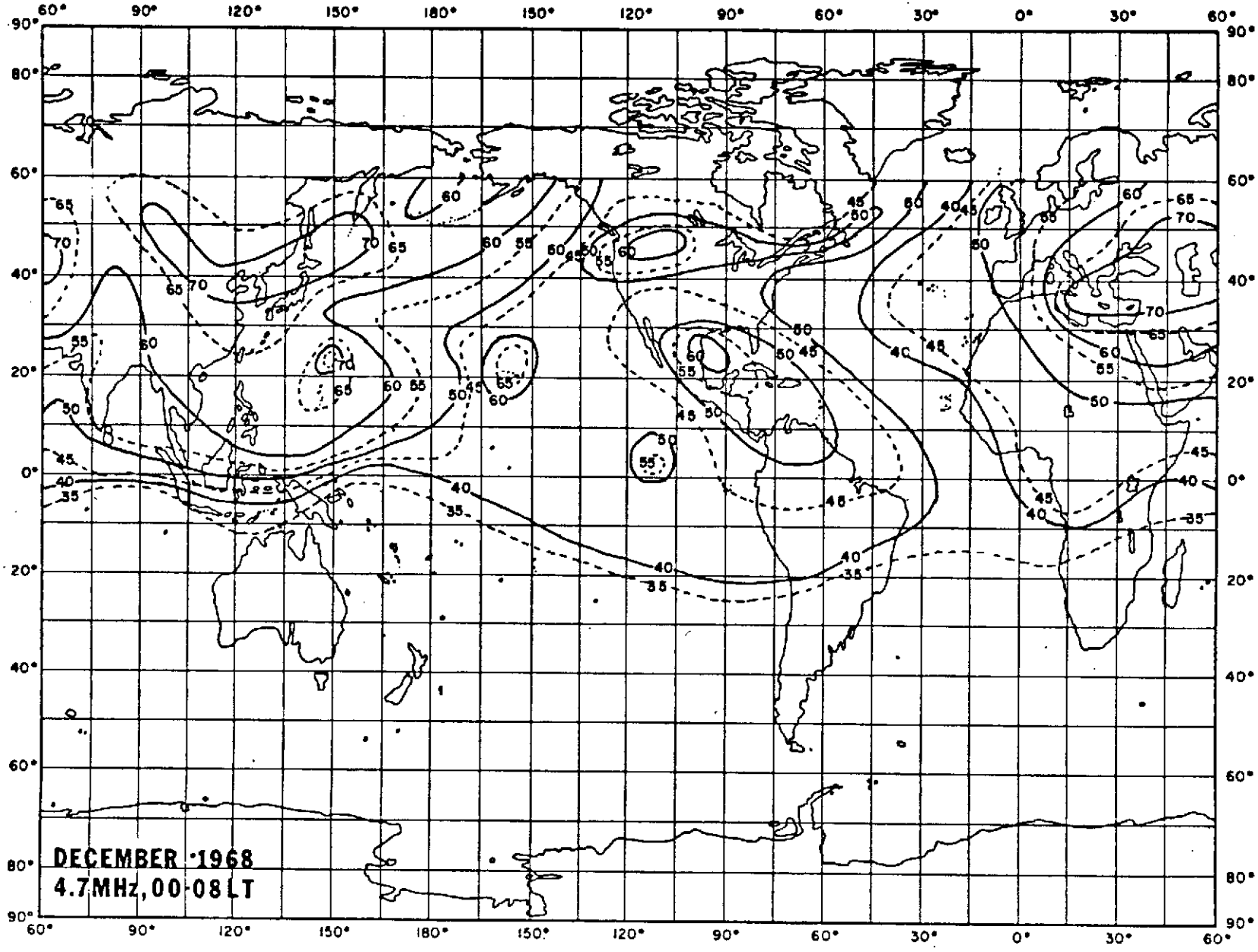

FIGURE 16

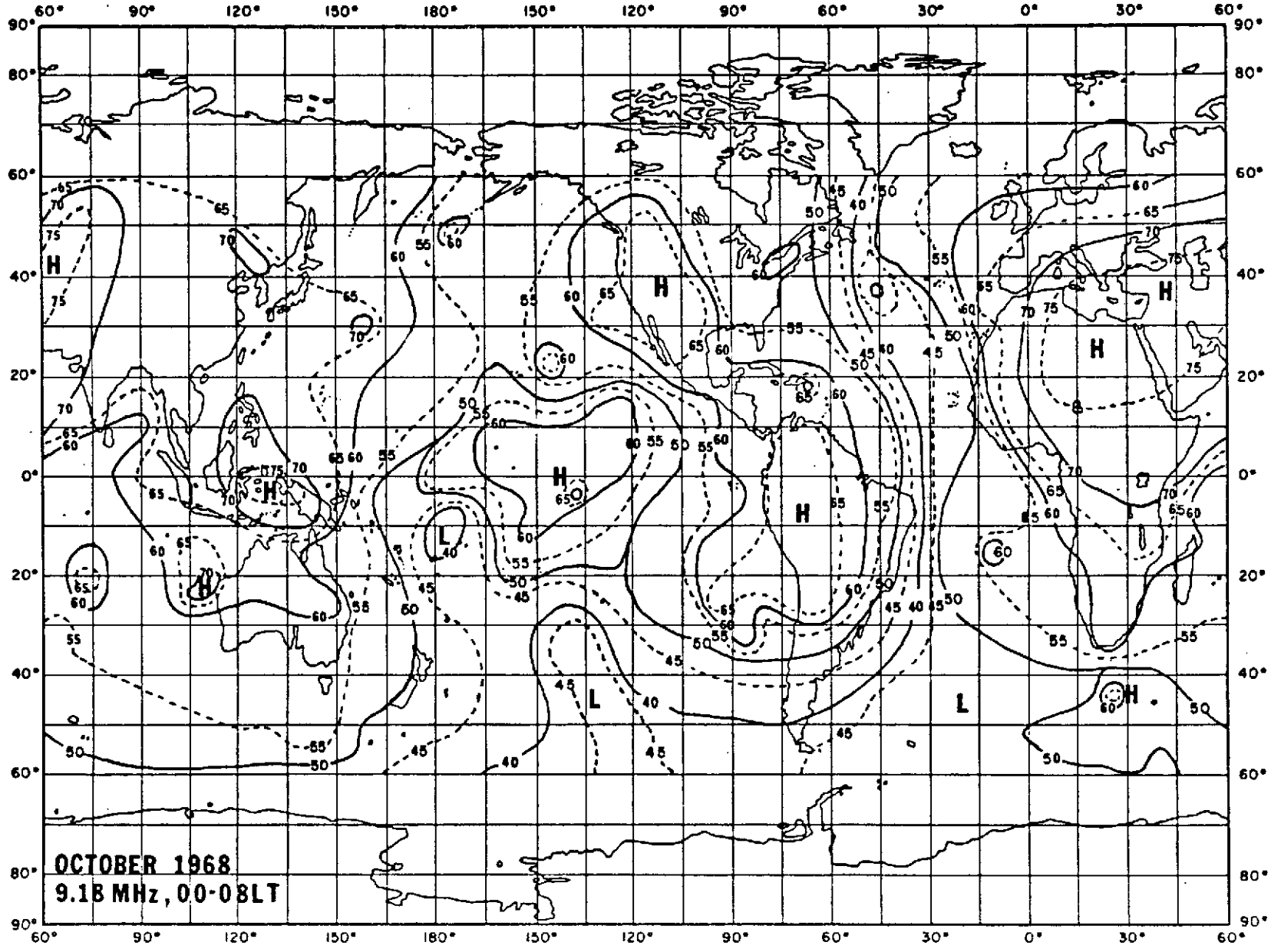

FIGURE 17

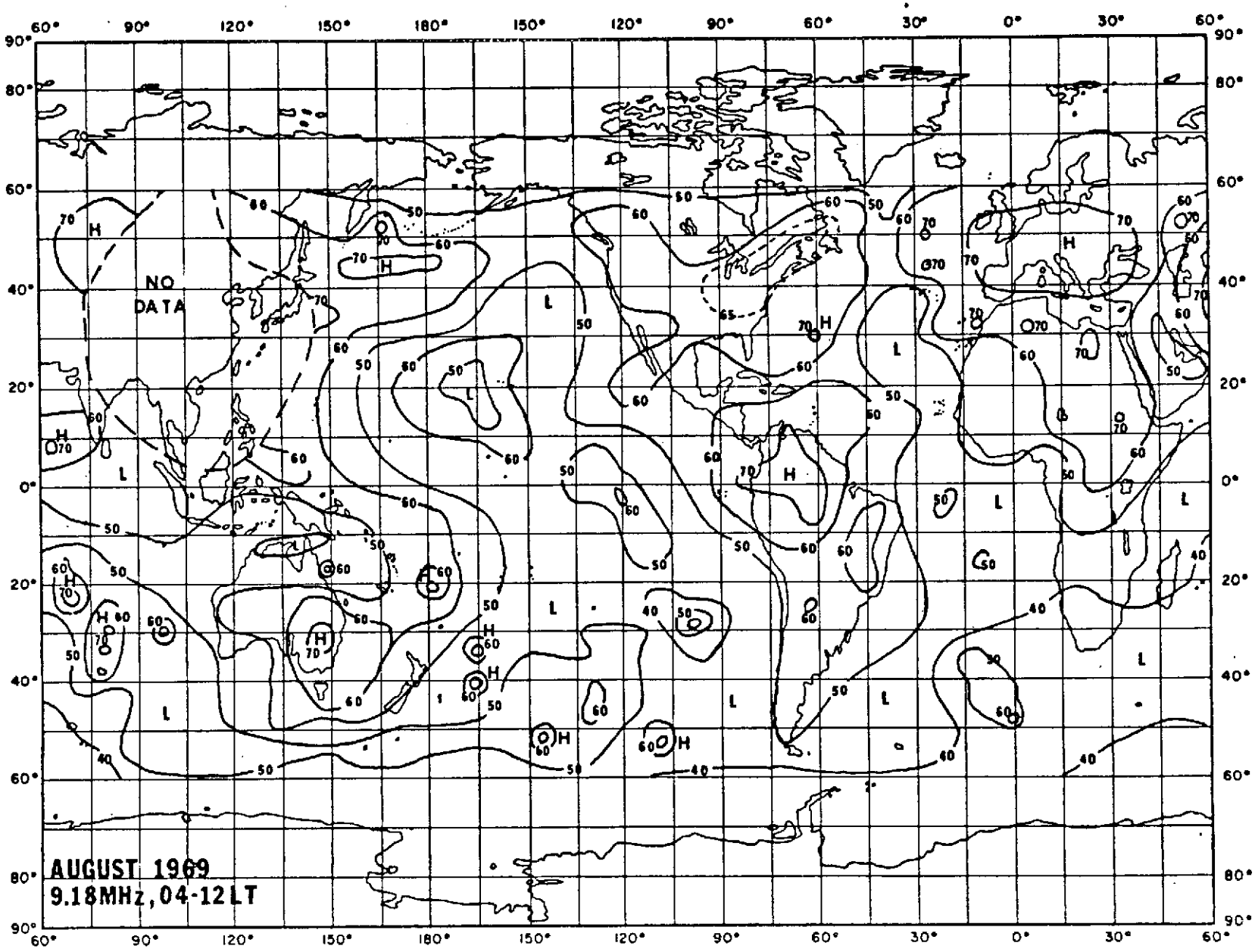

FIGURE 18

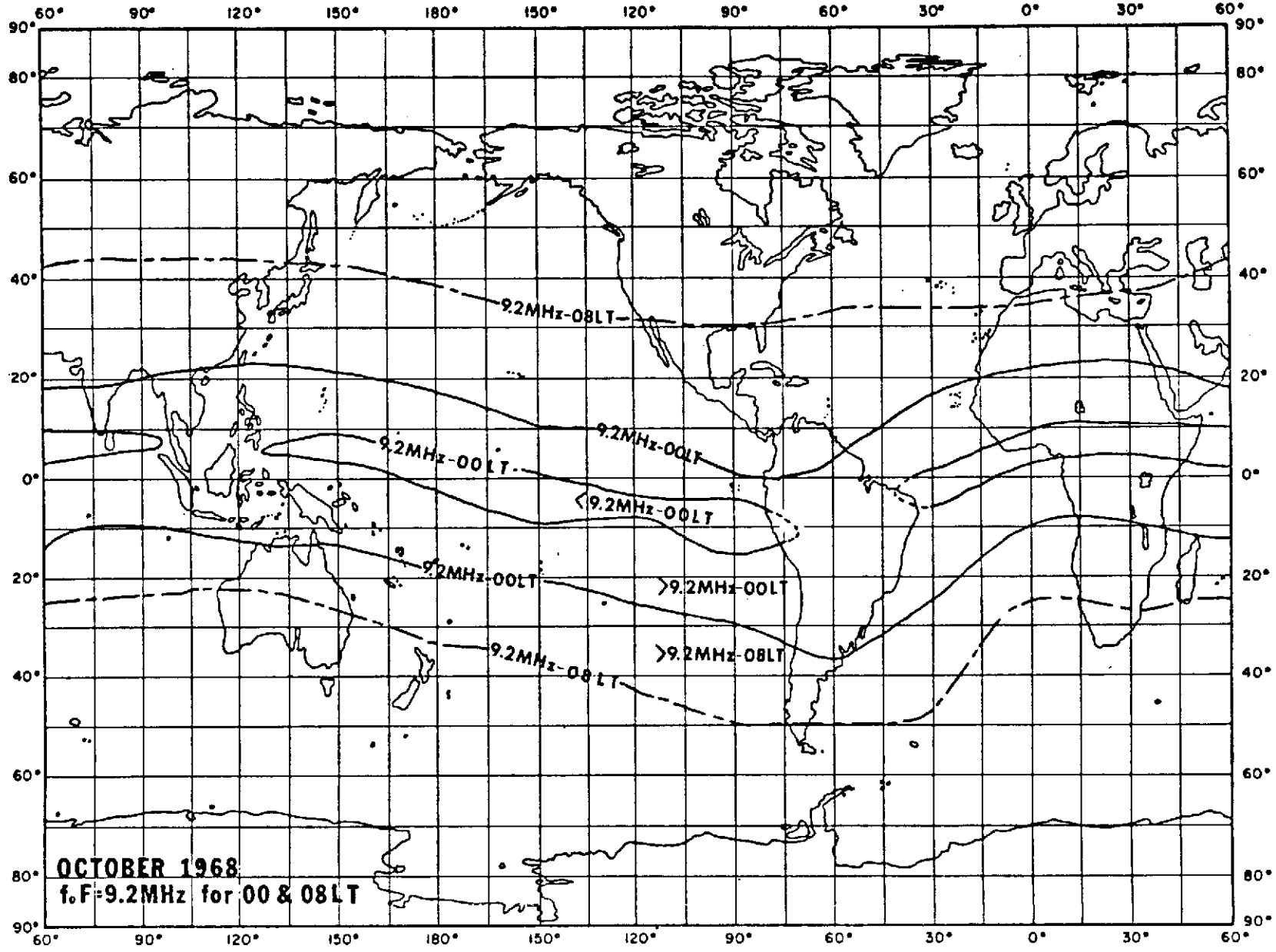
9.2MHz-08LT
9.2MHz-00LT
9.2MHz-00LT
9.2MHz-00LT
9.2MHz-00LT
9.2MHz-08LT
OCTOBER 1968
f₀F=9.2MHz for 00 & 08LT

FIGURE 19

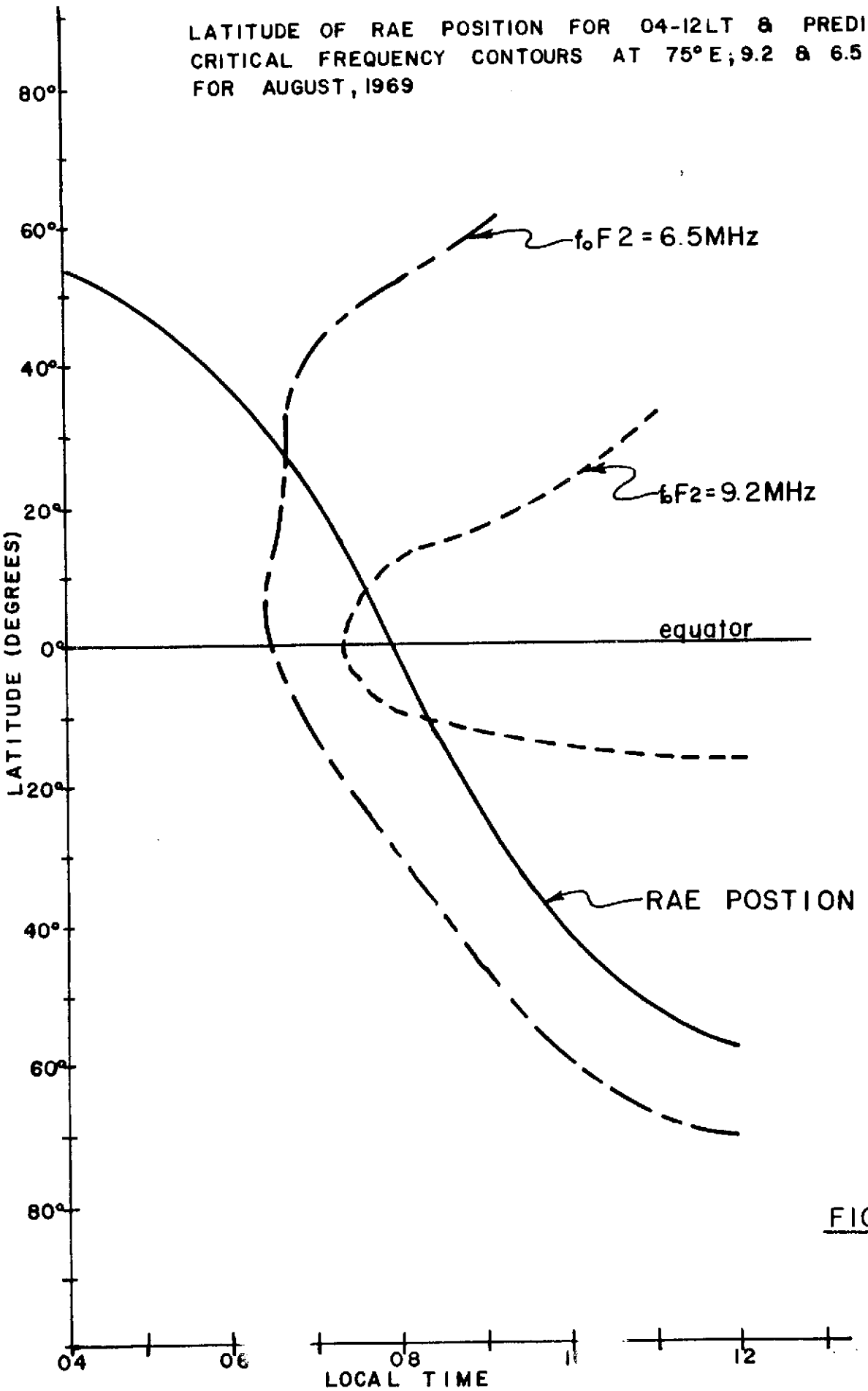
LATITUDE OF RAE POSITION FOR 04-12LT & PREDICTED CRITICAL FREQUENCY CONTOURS AT 75° E; 9.2 & 6.5 MHz FOR AUGUST, 1969
80°
60°
40°
20°
0°
20°
40°
60°
80°
LATITUDE (DEGREES)
foF2 = 6.5MHz
foF2 = 9.2MHz
equator
RAE POSTION
04
06
08
10
12
LOCAL TIME

FIGURE 20

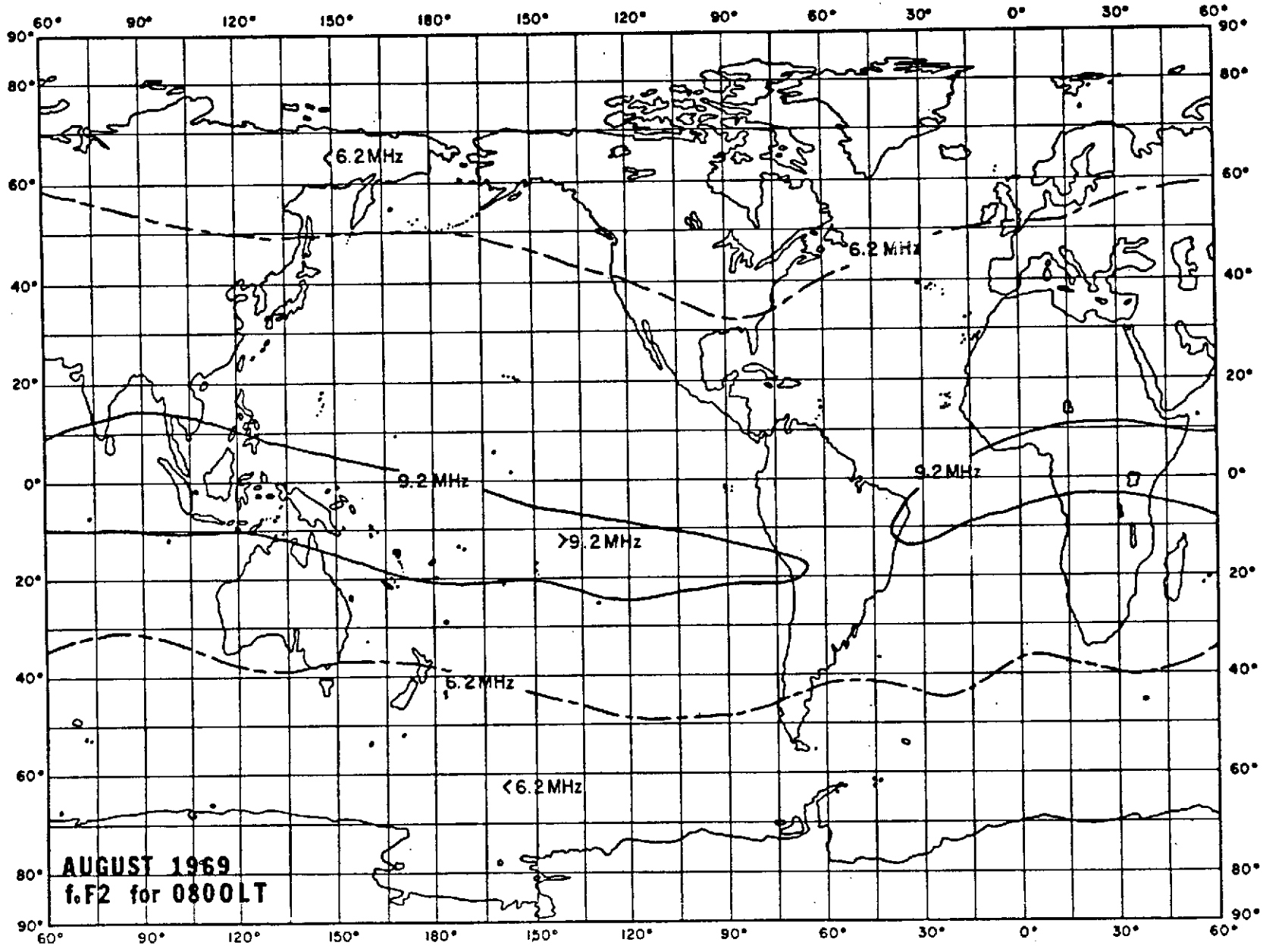
60° 90° 120° 150° 180° 150° 120° 90° 60° 30° 0° 30° 60°
90° 80° 60° 40° 20° 0° 20° 40° 60° 80° 90°
<6.2MHz
6.2 MHz
9.2 MHz
9.2MHz
>9.2 MHz
6.2MHz
<6.2MHz
AUGUST 1969
foF2 for 0800LT

FIGURE 21